

THE UNIVERSITY OF MICHIGAN
INDUSTRY PROGRAM OF THE COLLEGE OF ENGINEERING

THE STUDY OF NUCLEAR DECAY SCHEMES
BY THE SINGLE CRYSTAL GAMMA-SUMMING-METHOD
AND A 30-CHANNEL PULSE HEIGHT ANALYZER

Fang-Cher-Chang

A dissertation submitted in partial fulfillment
of the requirements for the degree of
Doctor of Philosophy in the
University of Michigan
1958

engn

UMRI200

ACKNOWLEDGMENT

I wish to express my deepest thanks to Professor Weidenbeck for his guidance and help during this research.

It is a pleasure to record here that the design of the main circuits of the apparatus is due to Dr. D. Lu and the construction of the apparatus is the joint effort of Dr. D. Lu, Dr. R. W. Lide and myself.

I am also grateful to Associate Professors William C. Parkinson and Robert W. Pidd for the use of the facilities of their Projects. Finally I wish to thank Mr. William Downer who made numerous bombardments for me.

TABLE OF CONTENTS

	<u>Page</u>
ACKNOWLEDGMENTS.....	ii
LIST OF FIGURES.....	v
I. INTRODUCTION.....	1
Nuclear States.....	1
General Properties of Nuclear Decay.....	3
Beta Decay.....	4
Gamma Emission and Internal Conversion.....	8
Some Remarks on Nuclear Models.....	11
Shell Model.....	11
Collective Model.....	15
II. EXPERIMENTAL METHODS.....	19
NaI(Tl) Scintillation Spectrometer.....	19
Introduction.....	19
Resolving Time and Energy Resolution.....	20
Counting Rate.....	22
The Construction of a Scintillation Spectrometer.....	25
Crystals.....	25
Photo-Multiplier and Associated Power Supply.....	26
Linear Amplifier.....	28
Multi-Channel Differential Analyzer.....	32
Decade Scaler.....	35
III. RESULTS.....	37
Cu ⁶² and C ¹¹	38
Co ⁵⁷	44
Rb ⁸⁶	46
Cr ⁵¹	50
Ta ^{182m}	52
Cl ³⁴	54
Dy ¹⁶⁵	58
Tc ⁹⁶	62
Ag ¹⁰⁸	65

TABLE OF CONTENTS CONT'D

	<u>Page</u>
Sm ¹⁵³	67
Conclusions.....	69
BIBLIOGRAPHY.....	70

LIST OF FIGURES

<u>Figure</u>		<u>Page</u>
1	The Gamma-Summing NaI(Tl) Counter.....	21
2	The Photomultiplier Power Supply.....	27
3	The Photomultiplier, Preamplifier, and the First Unit of the Main Amplifier Circuit.....	29
4	The Second Unit of the Main Amplifier Circuit.....	30
5	The Block Diagram of the Pulse Height Analyzer.....	31
6	The Pulse Height Analyzer Circuit.....	34
7	The Scaler Circuit.....	36
8	The Normal Gamma Spectrum of Cu ⁶²	39
9	The Sum Gamma Spectrum of Cu ⁶²	40
10	The Normal Gamma Spectrum of C ¹¹	41
11	The Sum Gamma Spectrum of C ¹¹	42
12	The Sum Gamma Spectrum of C ¹¹ with the Source Enclosed in a Copper Container.....	43
13	The Normal and Sum Gamma Spectra of Co ⁵⁷	45
14	The Normal Gamma Spectrum of Rb ⁸⁶	47
15	The Sum Gamma Spectrum of Rb ⁸⁶	48
16	The Normal and Sum Gamma Spectra of Cr ⁵¹	51
17	The Normal Spectrum of Ta ^{182m}	53
18	The Sum Gamma Spectrum of Ta ^{182m}	55
19	The Normal Gamma Spectrum of Cl ³⁴	56
20	The Sum Gamma Spectrum of Cl ³⁴	57
21	The Normal Gamma Spectrum of Dy ¹⁶⁵	59
22	The Sum Gamma Spectrum of Dy ¹⁶⁵	60

LIST OF FIGURES CONT'D

<u>Figure</u>		<u>Page</u>
23	The Sum Gamma Spectrum of Tc ⁹⁶	63
24	The Normal Gamma Spectrum of Ag ¹⁰⁸	64
25	The Sum Gamma Spectrum of Ag ¹⁰⁸	66
26	The Normal and Sum Gamma Spectrum of Sm ¹⁵³	68
27	Single Particle Shell Scheme	70

CHAPTER I
INTRODUCTION

Nuclear States

The hypothesis regarding nuclear constitution is that nucleus is made up of protons and neutrons. It is convenient to consider it as an unperturbed system. This is justified by the fact that the interaction between the atomic electrons and the nucleus is of electromagnetic nature and the strength of the interaction is measured by the charge of the electron ($e = 4.8 \times 10^{-10}$ esu). Being a bounded system its total energy can assume only discrete values. We shall call them energy levels and refer to the state with the lowest energy as the ground state, the state with the next higher energy the first excited state, and so on. A quantitative prediction of these energy levels is unattainable without the assumption of a specific nuclear model. On the other hand, a study of the energy level schemes can lead us to further understanding of the nuclear structure. Besides the total energy, other quantities are frequently used to characterize a nuclear state, such as, parity, spin (total angular momentum), lifetime, magnetic moment and quadruple moment. Of course, a complete characterization of a state requires $4A$ independent quantities ($A =$ mass number), since the nucleons inside a nucleus move more or less independently of each other and each nucleon has four degrees of freedom. In the absence of external forces, a (bare) nucleus will remain indefinitely in a certain state. However, the interaction between the nucleons and atomic electrons through the electromagnetic field may

cause transitions between states of the unperturbed system. The energy of a radiative state can not be determined exactly. The uncertainty in the energy, or level width, is related to the lifetime by the uncertainty relation: energy uncertainty \times lifetime $\sim h$. For states having lifetime as short as 10^{-17} seconds, the level width is of the order of 1 kev. By measuring the energies of the gamma rays and electrons emitted, a tentative energy level scheme can always be constructed. This is true at least for excited states as high as several mev above the ground state. At still higher energies, the level spacing gets smaller, the level width becomes wider, and eventually the discrete feature of energy levels is destroyed. This can be seen as follows: it is known that as a crude approximation, a nucleus can be treated as a system of independent particles moving in a square well potential. For simplicity, we consider a particle confined in a cubic finite volume with perfectly reflecting walls. Each state is characterized by three integral positive numbers. The number of states which lie between the energy range E and $E + \Delta E$ can be shown to be proportional to $E^{1/2}$. For a system of many particles, the crowding together of energy states at high energies will be more pronounced. At the same time the number of possible ways by which these high-lying states may decay increases, and consequently their level widths become broader.

Most excited states have a lifetime in the range 10^{-17} to 10^{-10} seconds. It has also been observed that occasionally excited states have much longer lifetimes. More than 120 examples are listed in "Tables of Isotopes" with lifetime ranging from 10^{-10} seconds to many years. Such

states are commonly called isomeric states. As a rule, the short-lived excited states decay by gamma emission and internal conversion only. Since internal conversion is a second order effect, gamma emission usually plays a dominant role. Hence gamma-gamma coincidence measurements can offer considerable information concerning energy level schemes.

General Properties of Nuclear Decay.

The binding energy of a nucleus is $ZM_p + (A - Z)M_n$ - mass of the nucleus where M_p and M_n are the masses of proton and neutron, respectively, and A and Z are the mass number and atomic number of the nucleus; it tends to assume a minimum value. Thus a nucleus in its ground state may still undergo decay of various modes.

All heavy elements are unstable against alpha decay; the lifetimes range from 10^{-21} seconds to 10^{15} years. Alpha emitters occur for $Z = 60$ (Nd^{144}), $Z = 62$ (Sm^{146} and Sm^{147}), $Z = 64$ (Gd^{148} , Gd^{149} , and Gd^{150}), $Z = 65$ (Tb^{149} and Tb^{151}), $Z = 78$ (Pt^{190}) and $Z = 83$ to 100.

Most other unstable nuclei decay by beta emission; the lifetimes lie between 0.02 seconds and 10^{11} years. Nuclear fission and nucleon emission are rarely observed. It should also be mentioned that the simultaneous emission of two or more particles is not very probable.

A consistent theory that can account for all the decay processes is at present out of the question. We shall have to be contented, for each particular case, with a phenomenological interpretation based on a few simple hypotheses, the correctness of which rests solely on its conformity with empirical results. We shall discuss only beta decay and

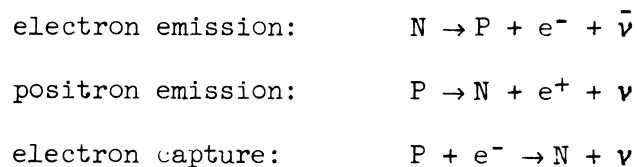
gamma emission in some detail, since they are the main concern in the study of energy level schemes.

In the standard perturbation theory, the transition probability per unit time of a transition from an initial state i to a final state f of the unperturbed system is

$$\frac{2\pi}{\hbar} | \langle f | H' | i \rangle |^2 \delta(E_f - E_i)$$

where H' is the interaction term in the Hamiltonian of the total system of the nucleus and atomic electrons, E_i and E_f are the energies of the states i and f , respectively, and the bracket denotes matrix element. δ is the Dirac delta function. As soon as the interaction term is found, the probabilities and selection rules of the decay process can be evaluated, provided the interaction is sufficiently weak.

Beta Decay-- Under this category, three processes are included, namely, electron emission, positron emission and electron capture. In the Fermi theory of beta decay, these processes are represented schemetically as follows:



with the assumption of a hypothetical particle ν , called neutrino, of negligible mass and spin $1/2$, as required by the conservation laws of angular momentum and energy. $\bar{\nu}$ denotes an anti-neutrino. The interaction which initiates the beta transitions is very weak with an interaction constant of the order 10^{-49} erg cm³. Thus the standard perturbation theory

is applicable. The beta transitions can be classified as allowed, once forbidden, twice forbidden, and so on. Each forbiddenness reduces the transition probability by a factor of about 100. The physical interpretation of this classification is that successively larger orbital angular momenta are carried away by the electron and neutrino. The lifetime of the radiative state depends on the character of the state as well as that of the state (or states) into which the transition leads. It can therefore vary over a wide range. The mere specification of spin and parity change puts little systematic restrictions on the value of the lifetime. However, the comparative half-life defined by

$$ft = (mc^2)^{-5} \int_{mc^2}^{E_0} F_{\pm}(Z, E_0)(E_0 - E)^2 (E^2 - m^2 c^4)^{1/2} E dE$$

where t is the half-life, E_0 is the maximum energy of the beta particle, and $F_{\pm}(Z, E_0)$ expresses the coulomb effect on the beta particle, is related to the spin and parity change in this way:

<u>Transition</u>	<u>Parity Change</u>	<u>Spin Change</u>	<u>Log (ft)</u>
allowed	no	0, 1	3 - 5
first forbidden	yes	0, 1, 2	7
second forbidden	no	0, 1, 2, 3	10
etc.			

In addition to the properties listed, allowed transitions yield straight lines on a Kurie or Fermi plot, that is, a plot of $(P(p)/Fp^2)^{1/2}$ versus E , where $P(p) dp$ is the probability of finding a beta particle with momentum between p and $p + dp$. Thus a knowledge of beta transitions may help us correlate the energy level schemes of adjacent atomic numbers and make spin, parity and level order assignments.

The interaction term H' for beta decay shall satisfy two requirements, relativistic invariance and agreement with experiment. Invariance means that H' remains unchanged under Lorentz transformation. If we assume that nucleons and neutrinos, like electrons, obey Dirac's equation, then they are described by four-spinors. We can form the following covariant quantities:

$$\begin{aligned}
 \text{Scalar} &= \psi^* \beta \varphi \\
 \text{4-vector} &= \begin{matrix} \psi^* \alpha_i \varphi & (\text{space components}) \\ i \psi^* \varphi & (\text{time component}) \end{matrix} \\
 \text{anti-symmetrical} \\
 \text{tensor} &= \begin{matrix} \psi^* \beta \sigma_i \varphi & (= \text{jkth component; } i, j, k \text{ cyclic}) \\ \psi^* \beta \alpha_i \varphi & (= \text{i4th component}) \end{matrix} \\
 \text{axial 4-vector} &= \begin{matrix} \psi^* \sigma_i \varphi & (\text{space components}) \\ i \psi^* \gamma_5 \varphi & (\text{time components}) \end{matrix} \\
 \text{pseudo-scalar} &= \psi^* \beta \gamma_5 \varphi \\
 i, j, k &= 1, 2, 3
 \end{aligned}$$

where ψ and φ are wavefunctions of the electron and anti-neutrino, respectively, α_i and β are Dirac matrices, and $\sigma_i = i\alpha_j\alpha_k$ (i, j, k cyclic). Analogous quantities can be formed if the initial and final wavefunctions of the nucleus are used instead of φ and ψ . The invariant interaction energy densities are:

$$\begin{aligned}
 H_S &= G_S (\Psi_f^* \beta \Psi_i) (\psi^* \beta \varphi) \\
 H_V &= G_V \left\{ (\Psi_f^* \Psi_i) (\psi^* \varphi) - (\Psi_f^* \vec{\alpha} \Psi_i) (\psi^* \vec{\alpha} \varphi) \right\} \\
 H_T &= G_T \left\{ (\Psi_f^* \beta \vec{\sigma} \Psi_i) (\psi^* \beta \vec{\sigma} \varphi) + (\Psi_f^* \beta \vec{\alpha} \Psi_i) (\psi^* \beta \vec{\alpha} \varphi) \right\} \\
 H_A &= G_A \left\{ (\Psi_f^* \vec{\sigma} \Psi_i) (\psi^* \vec{\sigma} \varphi) - (\Psi_f^* \gamma_5 \Psi_i) (\psi^* \gamma_5 \varphi) \right\} \\
 H_P &= G_P (\Psi_f^* \beta \gamma_5 \Psi_i) (\psi^* \beta \gamma_5 \varphi)
 \end{aligned}$$

where Ψ_i and Ψ_f are the initial and final wavefunctions of the nucleus, G 's are arbitrary constant, $\vec{\alpha} = (\alpha_1, \alpha_2, \alpha_3)$ and $\vec{\sigma} = (\sigma_1, \sigma_2, \sigma_3)$.

For parity-mixing beta interactions, we have five more invariant interaction energy densities. They are:

$$H'_S = G'_S (\Psi_f^* \beta \Psi_i) (\psi^* \beta \gamma_5 \varphi)$$

$$H'_V = G'_V \left\{ (\Psi_f^* \Psi_i) (\psi^* \gamma_5 \varphi) - (\Psi_f^* \vec{\alpha} \Psi_i) (\psi^* \vec{\alpha} \gamma_5 \varphi) \right\}$$

$$H'_t = G'_t \left\{ (\Psi_f^* \beta \vec{\sigma} \Psi_i) (\psi^* \beta \vec{\sigma} \gamma_5 \varphi) + (\Psi_f^* \beta \vec{\alpha} \Psi_i) (\psi^* \beta \vec{\alpha} \gamma_5 \varphi) \right\}$$

$$H'_a = G'_a \left\{ (\Psi_f^* \vec{\sigma} \Psi_i) (\psi^* \vec{\sigma} \gamma_5 \varphi) - (\Psi_f^* \gamma_5 \Psi_i) (\psi^* \varphi) \right\}$$

$$H'_p = G'_p (\Psi_f^* \beta \gamma_5 \Psi_i) (\psi^* \beta \varphi)$$

In these five types of interactions, the parity of the system of parent nucleus and anti-neutrino (or atomic electron) is different from the parity of the system of daughter nucleus and beta particle (or neutrino).

For each interaction type, the selection rules on spin and parity of nuclear states can be derived. However, a final evaluation of the beta transition probability requires a knowledge of nuclear structure. By comparing measure ft values with the predictions based on a specific nuclear model, we may obtain a test on the validity of the basic assumptions of the model.

Electron capture is expected to obey the same selection rules as beta emission, since the same kind of nuclear matrix element is involved. Positron emission and electron capture compete with each other, the former being more probable when E_0 is large and Z is small. In fact, very few positron emitters are found for large values of Z . For elements

with $Z \geq 83$, there is only one case of positron emission (Np^{234}) as compared to 82 cases of electron capture. The energies of positrons emitted by high Z isotopes usually lie in the range from 1 to 3 Mev.

Gamma Emission and Internal Conversion--The de-excitation of a nucleus can be accomplished by way of two different competing decay processes. It may emit a gamma photon, or an atomic electron may be ejected carrying away the energy of de-excitation. Pair formation is also possible if the energy of de-excitation is greater than $2 mc^2$ ($m =$ electron mass).

The Hamiltonian for a system of particles and electromagnetic field can be separated into a sum of three terms: the energy (kinetic + potential) of the particles in the absence of the radiation field, the energy of the radiation field, and the interaction energy between the particles and the radiation field. In the non-relativistic approximation, we obtain in the coulomb gauge for the interaction energy the expression:

$$H_{\text{int}} = - \sum_{\mathbf{k}} \left\{ \frac{e_{\mathbf{k}}}{m_{\mathbf{k}} c} (\vec{p}_{\mathbf{k}} \times \vec{A}(\vec{r}_{\mathbf{k}})) - \frac{e_{\mathbf{k}}^2}{2m_{\mathbf{k}} c^2} A^2(\vec{r}_{\mathbf{k}}) \right\} + \sum_{i>\mathbf{k}} \frac{e_i e_{\mathbf{k}}}{r_{i\mathbf{k}}}$$

where the $A^2(\vec{r}_{\mathbf{k}})$ term can be disregarded, for it belongs to processes of second order. It is also to be noted that we have excluded velocity-dependent forces among the particles which may bring in additional interaction terms.

Maxwell's electromagnetic theory gives the field equation:

$$\square \vec{A} \equiv \nabla^2 \vec{A} - \frac{1}{c^2} \frac{\partial^2 \vec{A}}{\partial t^2} = 0$$

with the Lorentz condition:

$$\text{div } \vec{A} = 0$$

It can be shown that \square commutes with the parity operator P and the angular momentum operator J defined by

$$\begin{aligned}
 P f(\vec{r}) &= f(-\vec{r}) \\
 \vec{J} &= \vec{L} + \vec{S}; \quad L^2 = -\frac{1}{\sin\theta} \frac{\partial}{\partial\theta} \sin\theta \frac{\partial}{\partial\theta} - \frac{1}{\sin^2\theta} \frac{\partial^2}{\partial\alpha^2} \\
 S_x &= \begin{pmatrix} 0 & 0 & 0 \\ 0 & 0 & i \\ 0 & i & 0 \end{pmatrix} \quad S_y = \begin{pmatrix} 0 & 0 & i \\ 0 & 0 & 0 \\ -i & 0 & 0 \end{pmatrix} \quad S_z = \begin{pmatrix} 0 & -i & 0 \\ i & 0 & 0 \\ 0 & 0 & 0 \end{pmatrix}
 \end{aligned}$$

The vector field A is therefore expressible in terms of the eigenfunctions of P, J^2 and J_z :

$$\vec{A}(\vec{r}) = \sum_{J,M} \vec{A}(J, M, \vec{r})$$

The component field with the parity eigenvalue $(-)^L$ is called the electric multipole field, and that with eigenvalue $(-)^{L+1}$ is called the magnetic multipole field. The multipole field belonging to the eigenvalue $L(L+1)\hbar^2$ of the operator J^2 is called a 2^L -pole field. In the classical language, an electric 2^L -pole field is produced by an oscillating electric 2^L -pole, and a magnetic 2^L -pole field by an oscillating magnetic 2^L -pole. In a transition caused by a 2^L -pole field, an angular momentum of $L\hbar$ units is radiated. In a way analogous to that used in beta decay, we classify the gamma transitions as follows:

Spin change	0	1	2	3
Parity change	E1, M2	E1, M2	M2, E3	E3, M4
No parity change	M1, E2	M1, E2	E2, M3	M3, E4

As photons have spin 1, $0 \rightarrow 0$ transitions cannot take place for gamma emission. Using the first term in H_{int} and the multipole expansion for

\vec{A} , we can calculate the probability for transitions of any multipole order by the perturbation method.

Internal conversion is supposedly brought about through an intermediate state for which the energy conservation law may be violated. There are two possible sets of intermediate states: (1) atomic electron remains in its original state; the nucleus goes to its ground state after the emission of photon. (2) the nucleus remains in its excited state; the atomic electron goes to a state in the continuum after the emission of a photon. In the coulomb gauge the coulomb interaction term in H_{int} is responsible for this two-step process. The probability for internal conversion is obtained with this term by perturbation calculations. If we make the approximation that the nuclear volume is negligibly small, we will find that the internal conversion coefficients and conversion ratios are quantities which are independent of any assumptions as regards nuclear models, for both internal conversion and gamma emission involve the same nuclear matrix element. (Internal conversion coefficient is defined as the ratio of the transition probability for internal conversion to that for gamma transition.) A crude approximation has shown that internal conversion is important for elements of high atomic number and transitions of low transition energy and high multipole order. The transition probabilities for both gamma emission and internal conversion decrease strongly with increasing multipole order. Usually it is only necessary to consider transitions of the lowest multipole order allowed by the selection rules. Sometimes radiations of both electric and magnetic multipole types are observed in the same transition, such as M1 and E2, and

E1 and M2. For internal conversion the same selection rules which hold for gamma emission apply with the only modification that $0 \rightarrow 0$ transitions are allowed.

The internal conversion coefficients and conversion ratios have been computed for many elements and transition energies by various authors. These provide us with a valuable means for making multipole order and parity assignment to the transition in question.

Some Remarks on Nuclear Models

In recent years, the shell model as proposed by Mayer and others and the collective model as proposed by Bohr and Mottelson have met great success in the explanation of many nuclear properties. We shall briefly review the fundamental assumptions of these theories and their implications in connection with energy level schemes.

Shell Model--The nucleons are treated as non-interacting, each moving in a common central potential field and with strong spin-orbit interaction. The Hamiltonian has the form:

$$H = \frac{p^2}{2m} + v(r) + f(r) \vec{s} \cdot \vec{l}$$

where \vec{s} and \vec{l} are the spin angular momentum and orbital angular momentum operators of the nucleon, and $f(r)$ is some function of r depending on the nature of the nuclear force. The stationary wavefunctions are of the form:

$$R_{nl}(r) Y_{jl \frac{1}{2}}^m$$

where $R_{nl}(r)$ satisfies the radial equation:

$$\frac{1}{r^2} \frac{d}{dr} \left(r^2 \frac{dR}{dr} \right) + \left[\frac{8\pi^2m}{h^2} (E - V(r)) - \frac{l(l+1)}{r^2} \right] R = 0$$

and $Y_{j\frac{1}{2}}^m$ is a simultaneous eigenfunction of the total angular momentum $\vec{j} = \vec{l} + \vec{s}$, its z-component, and the orbital angular momentum \vec{l} . Its explicit form is:

$$Y_{j\frac{1}{2}}^m(\theta, \varphi) = \sum_{m_l=1}^{\frac{1}{2}} \sum_{m_s=-\frac{1}{2}}^{\frac{1}{2}} C_{l\frac{1}{2}}(j, m; m_l m_s) Y_{lm_l}(\theta, \varphi) \alpha_{m_s}(s)$$

where Y_{lm_l} is an eigenfunction of the orbital angular momentum operator and α_{m_s} is an eigenfunction of the spin angular momentum operator, and $c_{l\frac{1}{2}}(j, m; m_l m_s)$ are constants. n, j, l, m are the total quantum number, total angular momentum quantum number, magnetic quantum number for total angular momentum and azimuthal quantum number, respectively, and assume the values:

$$n = 1, 2, 3, \dots$$

$$j = 1/2, 3/2, 5/2, \dots$$

$$l = 0, 1, 2, \dots$$

$$|m| \leq j$$

The schematic diagram of the nuclear levels shown in Appendix. Each state specified by n, l, j, m is $2j + 1$ - fold degenerate. Because of the coulomb force the proton level lies higher than the neutron level. Moreover, for protons, orbits of higher l are favored, because orbits of lower l penetrate deeper into the charged nuclear core.

The following coupling scheme is then adopted: (1) An even number of equivalent protons or neutrons (with same n and l) with the

same j couple to zero angular momentum. We therefore get the following result for the ground state of even-even nuclei: 0 spin and even parity. No exception to this rule has been found. (2) An odd number of equivalent protons or neutrons with the same j couple to an angular momentum j . It follows that the ground state spin of even odd nuclei is equal to the angular momentum of the odd particle and the parity is odd or even according as l of the odd particle is odd or even. A few exceptions to this rule has been observed. Na^{23} , Ti^{47} , Mn^{55} , and Se^{79} have ground state spin $j - 1$, instead of j . A third coupling rule is needed to explain the higher magic numbers; namely, 28, 50, 82, and 126. (3) The spin-orbit coupling splits the levels $j = l + 1$ and $j = l - 1$ with the former lying lower than the latter. This splitting increases with increasing values of l . An additional coupling rule describes how closely neighboring levels should be filled. It assumes that a negative potential energy is connected with double occupancy of a level. This energy is called the pairing energy and is an increasing function of l . For example, the nucleus Br^{79} with 35 protons should have a ground state spin $5/2$. However, the pairing energy favors the occupancy of the level $1f\ 5/2$ by the proton pairs, leaving the $2p\ 3/2$ level for the unpaired proton. The configuration becomes 3 protons in $2p\ 3/2$ level and 4 protons in $1f\ 5/2$ level in addition to closed shell protons, in spite of the fact that the $2p\ 3/2$ level is lower than the $1f\ 5/2$ level.

For odd-odd nuclei, no simple coupling rules could predict the ground state spin and parity.

As for the first excited states of even-even and even-odd nuclei, the parity of any state can be found if the nucleon configuration is given. In our picture of independent nucleons, the total wavefunction is the product of individual wavefunctions each containing the coordinates of one nucleon. The resultant parity is the product of the individual parities of the individual wavefunctions. The spins of the excited states, in general, can not be rigorously derived. Even if Pauli's principle is taken into account, the nucleons in incompletely filled levels could couple their spins in various ways. By way of illustration, we consider ${}_{38}^{88}\text{Sr}_{50}$. The neutrons form a closed shell. The protons fill the levels $3p\ 3/2$ and $4f\ 5/2$ completely. The excited states should be a result of the excitation of a proton to a vacant level. $3p\ 1/2$ is the first vacant level. The excitation of a proton from either $3p\ 3/2$ or $4f\ 5/2$ to this level gives rise to a state of even parity. The measured character of the first excited state of ${}_{38}^{88}\text{Sr}$ at 1.85 Mev is $2+$. Hence, the spin is also compatible with the shell model expectation.

Another evidence which supports the shell model is the occurrence of islands of isomers. Isomers are defined as nuclides that can exist in its excited states for a long time. It has been observed that for odd A nuclei, isomers occur where the number of odd group of protons or neutrons is between 38 and 50, 64 and 82, and 100 and 126. This phenomenon is caused by the competition of two close-lying energy levels differing by three or more units of spin. The large spin change in the transition is responsible for the long lifetime. The level order based

on the shell model explain not only the regions where the isomers fall but also the multipole type of the transition involved.

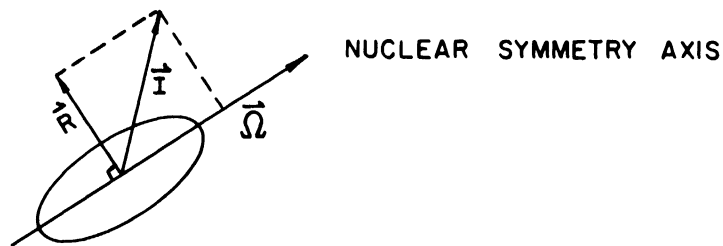
The shell model has also successfully predicted l - forbidden transitions in beta decay. These transitions are characterized by a change in the orbital angular quantum number l . Without the additional l -selection rules, many beta transitions would be classified as allowed transitions in contradiction to observations.

However shell model fails to explain the large quadruple moments of nuclei in the region $155 < \text{mass number} < 180$. Nor can it account for the occurrence of gamma transitions of electric quadruple type of very short lifetimes.

Nevertheless it is believed that the shell model constitutes a starting point in formulating a good nuclear model. The next step is to bring the internucleon interaction into the theory.

Collective Model--In the shell theory, the nucleons in closed shells contribute to an average static potential field; the energy levels are to be interpreted only as excitations of nucleons not in closed shells. The inadequacy of this procedure led us to take into consideration the dynamical behavior of the nuclear core. As soon as the core is treated as deformable, its number of degrees of freedom is enormously increased. A simple hypothesis is to assume the core to be an irrotational and incompressible flow of matter. With increasing number of nucleons outside of the core, the deformation of the core gets large on account of the polarizing effect of the former. The core in general possess axial symmetry for large deformations. For states of low excitation energies

(below 1 Mev, say), the assumption is made that the nucleons in non-closed shells move rapidly in their orbits around the core and the core performs slow surface oscillations (strong coupling approximation). The total angular momentum of the nucleus is shared among the core and the odd nucleons; to be more precise, the sum of the projections along the symmetry axis of the spins of the odd nucleons adds to the spin vector \vec{R} of the core to form the total angular momentum. A schematic diagram of this coupling follows.



Bohr and Mottelson have given the following expressions for the energies of rotational states:

(1) For even-even nuclei

$$E_{\text{rot}} = \frac{\hbar^2}{2J} I(I + 1)$$

$I = 0, 2, 4, \dots$ even parity

(2) For odd-even nuclei

$$E_{\text{rot}} = \frac{\hbar^2}{2J} \{ I(I + I_0(I_0 + 1)) \}$$

$I = I_0, I_0 + 1, I_0 + 2, \dots$

same parity as ground state

If $\Omega = 1/2$, an extra term is to be included in the above energy expression and the simple sequence of states is spoiled. J is the moment of inertia about an axis perpendicular to the symmetry axis.

Evidence for the existence of rotational spectrum has been found in numerous cases, especially in the region $155 < \text{mass number} < 185$. Rotational (excited) states have distinct properties: (1) They have the same parity as the ground state and the spin difference of adjacent states is either 1 or 2. (2) E 2 transition probabilities are greatly enhanced. And (3) they conform to some simple energy ratios and branching ratios of beta or gamma decay from any state to different members of a rotational band.

Scharff-Goldhaber and Weneser studied the first and second excited states of the even-even nuclei in the region $66 < \text{mass number} < 150$. They found the following regularities in the empirical data. (a) The character of the first excited states is commonly $2+$, and that of the second excited states is commonly $2+$, occasionally $0+$, $4+$, and odd spin and odd parity. (b) The energy ratio of the second to the first excited state fluctuates around 2.2. (c) Enhanced quadruple radiations are emitted during the second to the first excited state transition as well as the first to the ground state transition. Since this region is immediately adjacent to the rotational region, the existence of vibrational states is suggested. These facts can be interpreted in terms of small vibrations of the nuclear surface around the spherical equilibrium shape. Calculations based on the collective model give the following scheme for the first three vibrational states:

2E ----- $0+$, $2+$, $4+$
E ----- $2+$
o ----- $0+$

The second excited state is a degenerate triplet. The qualitative agreement between experiment and theory is good.

In conclusion, the collective model explains the regularities exhibited in quadruple moment and energy of the first and second excited states and enable us to classify nuclear energy levels as both particle and collective excitations. In view of the simple hypothesis that is adopted in the theory, it is not surprising that little quantitative success can be cited.

CHAPTER II
EXPERIMENTAL METHODS

NaI(Tl) Scintillation Spectrometer

Introduction--The main features of the NaI crystal are summarized:

1. It has a relatively short decay time - about 0.25×10^{-6} seconds. Theoretical calculations show that resolving times as low as 10^{-9} seconds are obtainable.
2. There is a linear relationship between incident gamma ray energy and output pulse height, at least between the energy range 0.5 kev to 6 mev.
3. It is more efficient in converting absorbed energy into light photons than any other phosphors known at present.
4. Monoenergetic gamma rays give rise to well-defined "photopeaks" in the pulse height distribution. For NaI contains 85% by weight of iodine and the absorption coefficient for photoelectric effect increases as the fourth power of the atomic number.

One disadvantage is its poor energy resolution. For a two inch diameter by two inch height crystal the half-width of the peak at 664 kev is about 9 per cent of the energy of the peak. It therefore, does not offer a high degree of accuracy in energy determination.

A schematic diagram of the NaI(Tl) counter is shown in Figure 1.

The physical processes involved are now briefly described. An incident gamma photon transfers the whole or part of its energy to

electrons within the phosphor by one of the three processes: (1) photo-electric effect, (2) Compton scattering, and (3) pair formation. Part of the absorbed energy is emitted as light photons, with a decay time characteristic of the phosphor. When these photons fall on the cathode of the photo-multiplier tube, photo-electrons are ejected. The number of photo-electrons are then multiplied at the dynodes of the photo-multiplier. The final electron avalanche arrives at the anode and gives rise to a voltage pulse, which is to be amplified to some magnitude suitable for triggering the pulse height analyzer.

Resolving Time and Energy Resolution

Resolving Time--The output pulse from the phosphor appears only at some time after the occurrence of the initial ionizing event. It is this time lag which sets the lower limit of the resolving time, since it can only be determined statistically. The chances of resolving two light pulses separated by a time interval smaller than the resolving time are slim. Thus if two gamma photons enter the crystal within a time shorter than the resolving time, a photopeak will be formed at an energy equal to the sum of the energies of the two gamma photons. This fact will later be used in the analysis of the gamma spectra taken in this study. It has been shown that for the presently known phosphors the limit of resolving time is probably 3×10^{-10} seconds. Furthermore, the time for light collection at the cathode of the photo-multiplier and the transit time of electrons through the photo-multiplier also add to the uncertainty in the occurring time of the initial ionizing event. Because of the discharging and recharging of the capacitors and

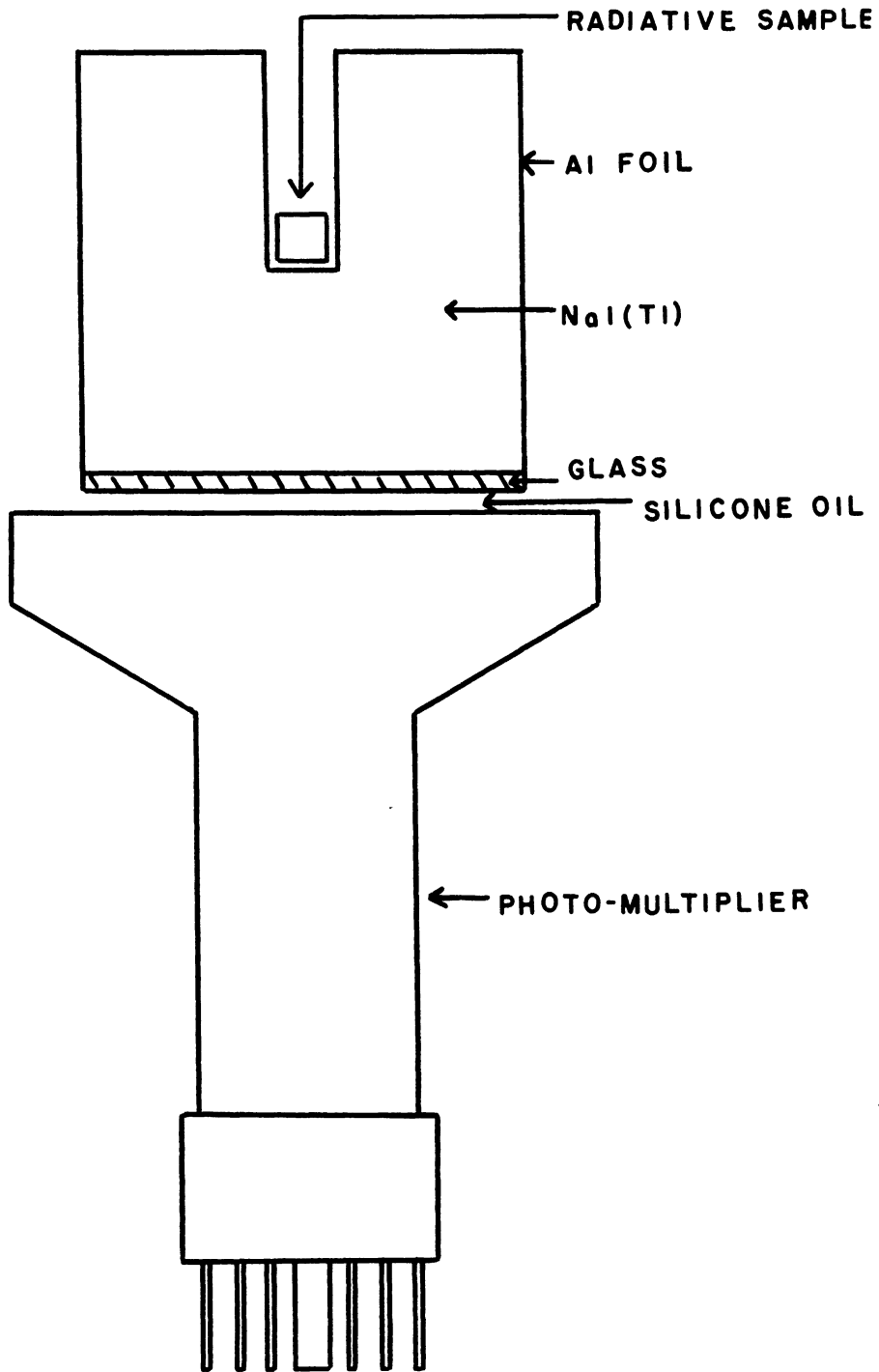


Figure 1. The Gamma-Summing NaI(Tl) Counter

stray capacitances present in the electronic circuit, a certain time interval following the triggering is needed to allow the circuit to return to its initial conditions. If two pulses arrive within an interval smaller than the rise time of the amplifier, the amplifier would tend to overload and the second pulse would not be amplified faithfully. As for the discriminator, a certain time must elapse following a previous pulse before it can respond to a second pulse. This time which is required for the recovery of the circuit can be taken as a measure of the resolving time of the circuit. The overall resolving time of the detecting system will be discussed in the following section.

Energy Resolution--The factors contributing to the fluctuations in the magnitude of the output pulses of a monoenergetic gamma photon are, first, variations in the intensities of light emitted at different locations inside the phosphor and variation in light transmission through the phosphor, secondly, nonuniform response over surfaces of cathode or dynodes and the small number of electrons involved in the first few stages of the photo-multiplier, and last, random noises in the amplifier and hum in the photo-multiplier power supply. It is seen that improvements in energy resolution can often be sought in the selection of crystals and photo-multipliers and the design of the amplifier and high voltage supply circuits. Large phosphors generally have poorer energy resolution than small ones. although the latter are less efficient in detecting high energy gamma rays.

Counting Rate--In order to minimize the counting loss and false discrimination of pulse amplitudes, we wish to know the overall resolving time of the

detecting system. The present apparatus consists of a sequence of components, containing a NaI counter, a linear amplifier, a discriminator and thirty scalers. The discriminator has a resolving time of about 4 microseconds, which is larger than the resolving times of the other components. Following the discussions on efficiency of counters by Ruark and Brammer, we now show that overall resolving time is approximately that of the discriminator, and get some idea as to the fastest counting rate permissible for the present apparatus if a 1% counting error can be tolerated.

We assume that the counting rate is sufficiently slow so that the chances of a pulse arriving during the recovery time of the counter and amplifier are negligible. Let the resolving time of the counter and amplifier be denoted by t_c and that of the discriminator by t_d . The average rate of pulses delivered by the amplifier is

$$f (1 - ft_c) \text{ pulses per unit time}$$

where f is the average rate of incoming particles over an interval when the detecting system is turned on. Of these pulses only those which are separated by at least $t_d - t_c$ will be correctly sorted by the discriminator. We have of course assumed that t_d is greater than t_c . The probability that no pulse occur in an interval after a previous pulse is

$$\exp (-f(t_d - t_c))$$

The product of the two expressions then gives the counting rate of the whole detecting system. The scaler does not enter the discussion, for it recovers after a count even before the discriminator does. We therefore have

$$\text{counting rate} = f (1 - ft_c) \exp (-(t_d - t_c))$$

If ft_d is also small compared to one, we obtain approximately

$$\text{counting rate} = f (1 - ft_d),$$

neglecting terms of higher order than ft_d . A 1% accuracy requires that the counting rate be no higher than 2500 counts per second.

When the source is placed inside the crystal, the crystal serves as a coincidence detector. Two particles which enter the crystal within its resolving time will be recorded as coincident. We shall employ the following notations.

N = number of disintegrations produced by the radioactive source per second.

N_i = number of counts per second actuated by particles of type i ($i = 1, 2$).

E_i = efficiency of the crystal for the detection of particles of type i ($i = 1, 2$).

N_{12} = real coincidence counts per second recorded by the crystal.

If the incoming particles are randomly distributed in time, we have the following relations:

$$N_1 = NE_1, N_2 = NE_2, N_{12} = NE_1E_2$$

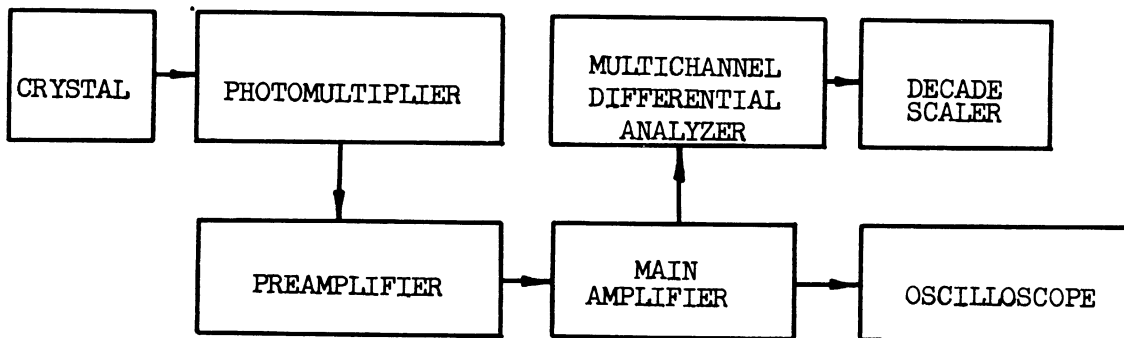
In addition, any two uncorrelated particles which happen to enter the crystal within its resolving time will give rise to accidental coincidence counts. The accidental coincidence rate is given as $2TN_1N_2$, T being the resolving time of the crystal. The accidental rate obviously should not be larger than the real rate. If the accidental rate is set equal to the real rate, we obtain the upper limit to the source strength as $1/2T$. By taking T to be 3×10^{-10} seconds, the limit is found to be 40 millicuries. In our apparatus the discriminator would become blocked before this limiting strength is reached. For fast single crystal summing

system, it is expected that the resolving time of the crystal will constitute the actual limit of the source strength.

The back-scattered photons also contributes to accidental coincidence rate. If the geometry of the experimental setup is such that the back-scattered photons are centered around a single energy, a false peak may appear in the spectrum. There are further contributions to the accidental coincidences from background radiations, and, if the source is a beta-emitter, from the beta particles emitted by the source. These however, give rise to a smooth distribution which may obscure weak photopeaks.

The Construction of a Scintillation Spectrometer

A block diagram of the spectrometer is as follows:



Crystals--A cylindrical hole of 1/4 inch diameter was drilled along the axis, so that the radioactive sample can be placed at the center of the crystal to produce summing effect. The occurrence of summing is explained by the fact that the nuclear life time against radioactive transitions is of the order of 10^{-13} seconds. Thus two gamma rays related by such a transition will be recognized by the crystal as simultaneous and a single

photopeak corresponding to an energy equal to the sum of the energies of the two gamma rays will be produced. Since the crystal must be protected against moisture, one end of the crystal is covered with glass and the remaining part of the surface is first coated with a layer of MgO powder and then sealed in an aluminum can. MgO powder provides better light reflection. The crystal is coupled to the top surface of the photomultiplier with silicone oil for good optical contact. NaI (Tl) crystal of three different sizes including 2 inch diameter by two inch height, 3 inch by 3 inch, and 5 inch by 4 inch, were used. The 2 inch by 2 inch one was found most satisfactory in so far as energy resolution and summing effect are concerned. The 5 inch by 4 inch one was used to detect weak summing at energies beyond one mev.

Photomultiplier and Associated Power Supply--A Dumont 6364 type photomultiplier was used. The potentials between the dynodes can be varied between 90 to 140 volts by adjusting a variable resistor in series with the power supply. The higher potential between the first dynode and the cathode improves energy resolution. The photomultiplier was shielded with mu-metal against outside magnetic field.

In a voltage-stabilized power supply, the stability of output voltage depends on the stability of the reference voltage. Higginbotham found that 5651 VR tube is satisfactory as regards voltage drift and temperature coefficient. The circuit shown in Figure 2 is a modified form of the one designed by him. A half-wave voltage doubler furnishes the high voltage to be stabilized. The usual regulating device employing a difference amplifier was used to stabilize both the high and low

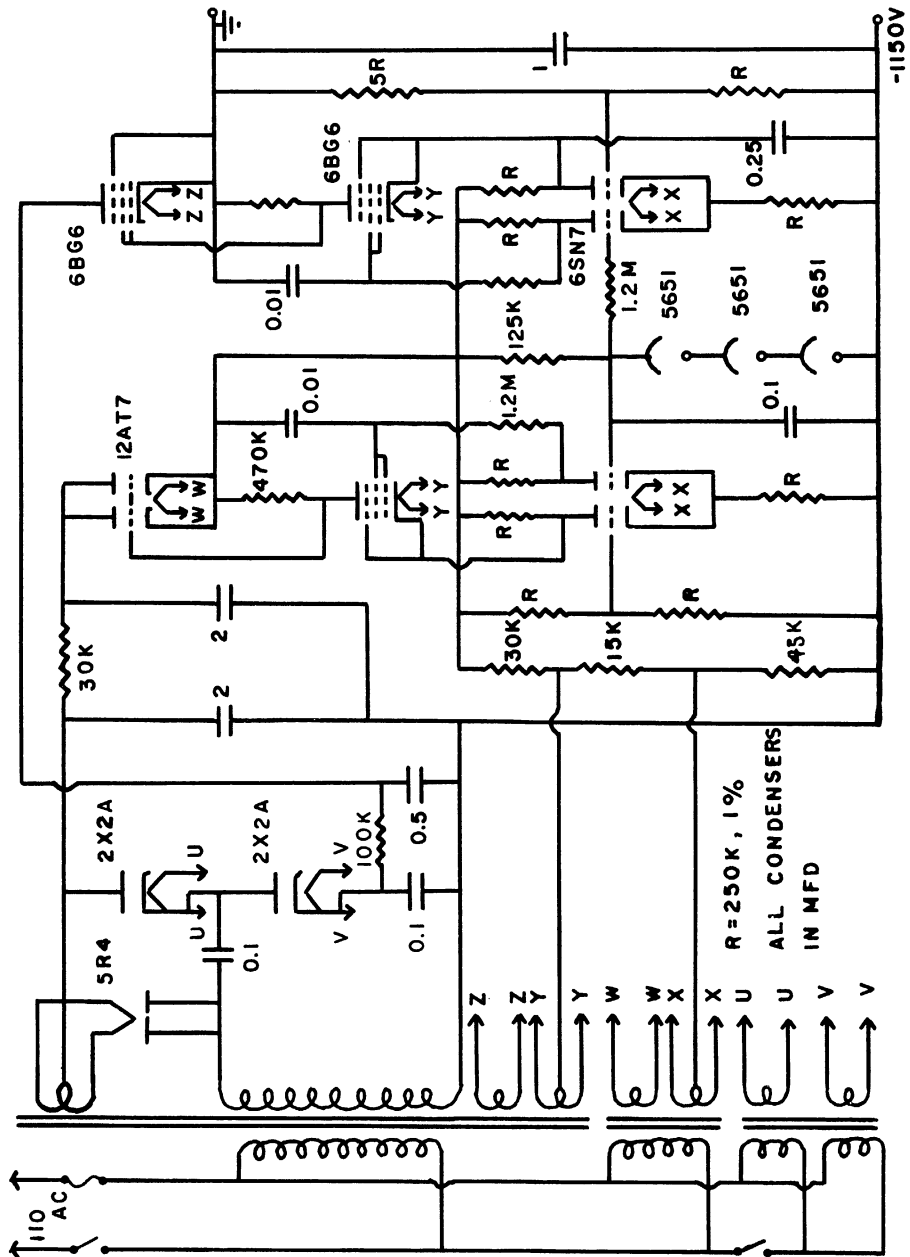


Figure 2. The Photomultiplier Power Supply

voltages. It is capable of delivering 2 ma at -1500 volts. The peak value of the ripple voltage is less than 0.03 volts and the voltage drift is less than 0.1% for long periods.

Linear Amplifier.--The linear amplifier is divided into three parts, a preamplifier with a gain of about one, and two amplifying units with (maximum) gain of about 50 each, all connected by RG-62/U coaxial cables. Besides the usual requirements for a good linear amplifier: linearity, stability and fast rise time, for pulse height analysis it is also necessary that the amplifier does not overload easily. If grid current flows after a large positive pulse, the coupling condenser will be charged and the grid bias will be shifted. With an amplifier of not more than three amplifying stages linearity and stability can be easily achieved by negative feedback. The rise time is determined by the load resistance and the total load shunt capacitance of the various stages of the amplifier. Figure 3 shows the preamplifier and the first part of the main amplifier, and Figure 4 shows the second part of the main amplifier. The preamplifier also serves to invert the phase of the pulse from the photo-multiplier. The rise time of each unit of the amplifier is about 0.1 microseconds. When the discriminator bias is set for analysis of small pulses, the presence of large pulses is undesirable. For the purpose of clipping the positive signal at the input of the second unit of the main amplifier, a clipper circuit using a 6AH6 tube is connected with the grid assuming one of the three different D. C. potentials depending on the discriminator bias setting such that the input signal after amplification does not overload the trigger tubes.

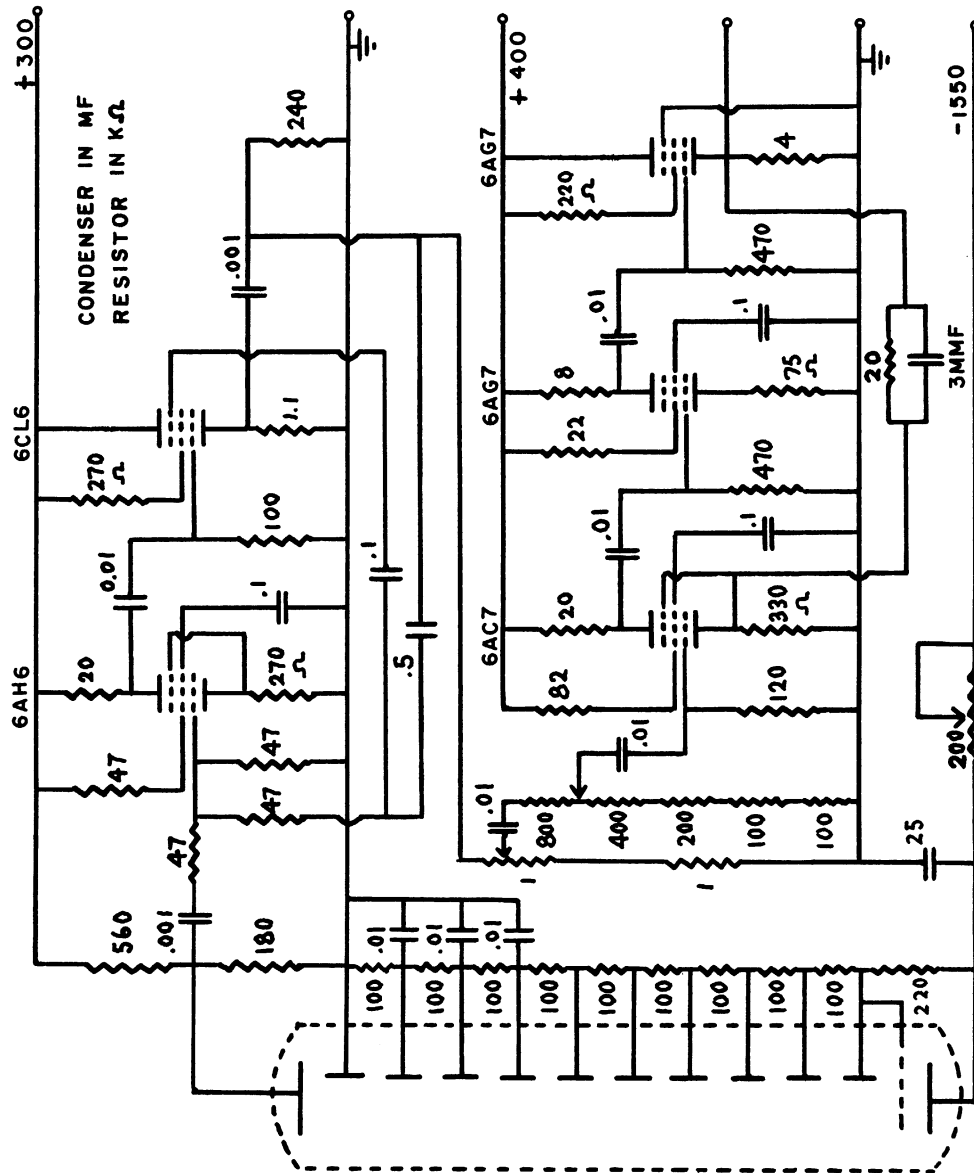


Figure 3. The Photomultiplier, Preamplifier, and the First Unit of the Main Amplifier Circuit

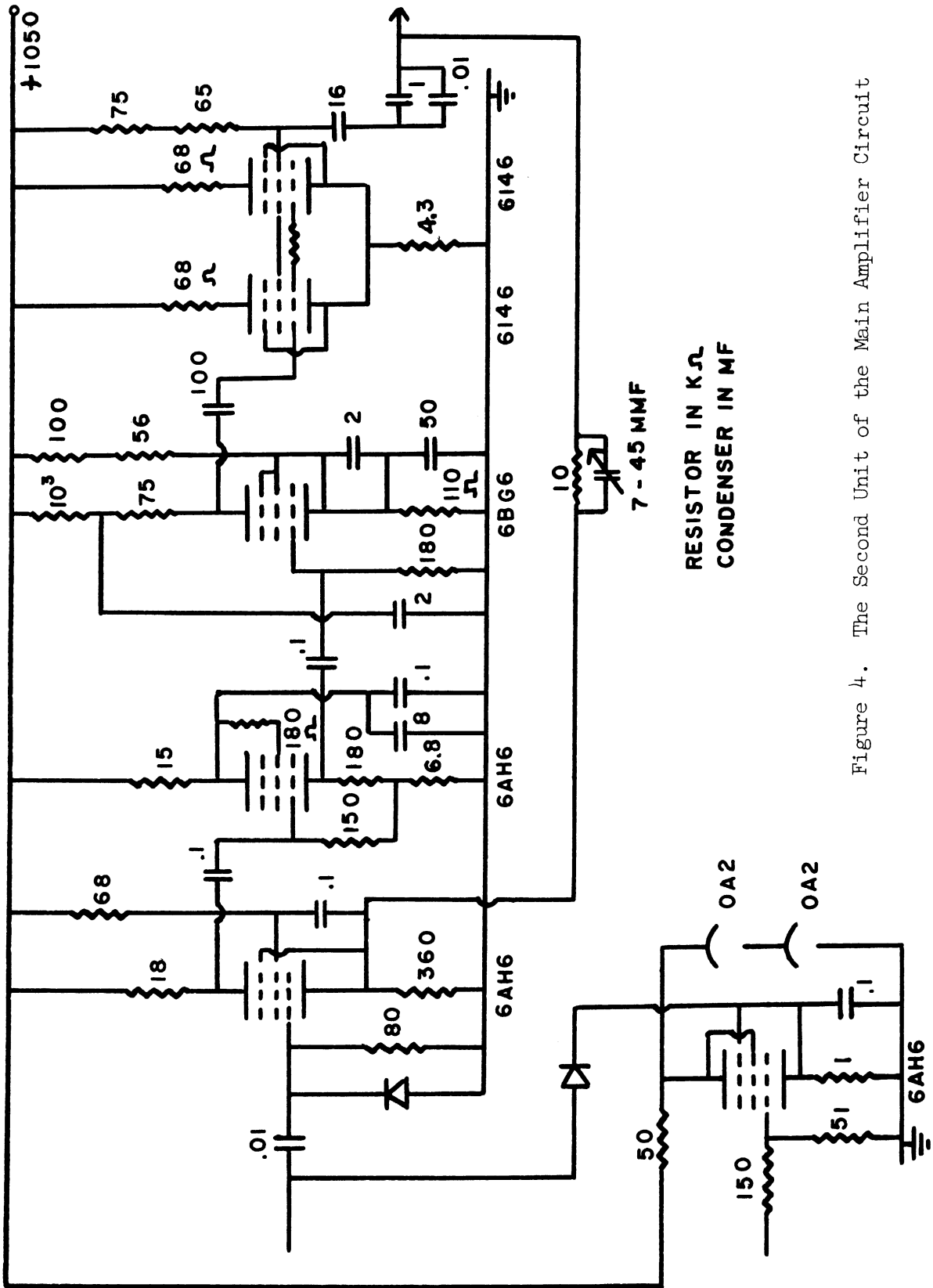


Figure 4. The Second Unit of the Main Amplifier Circuit

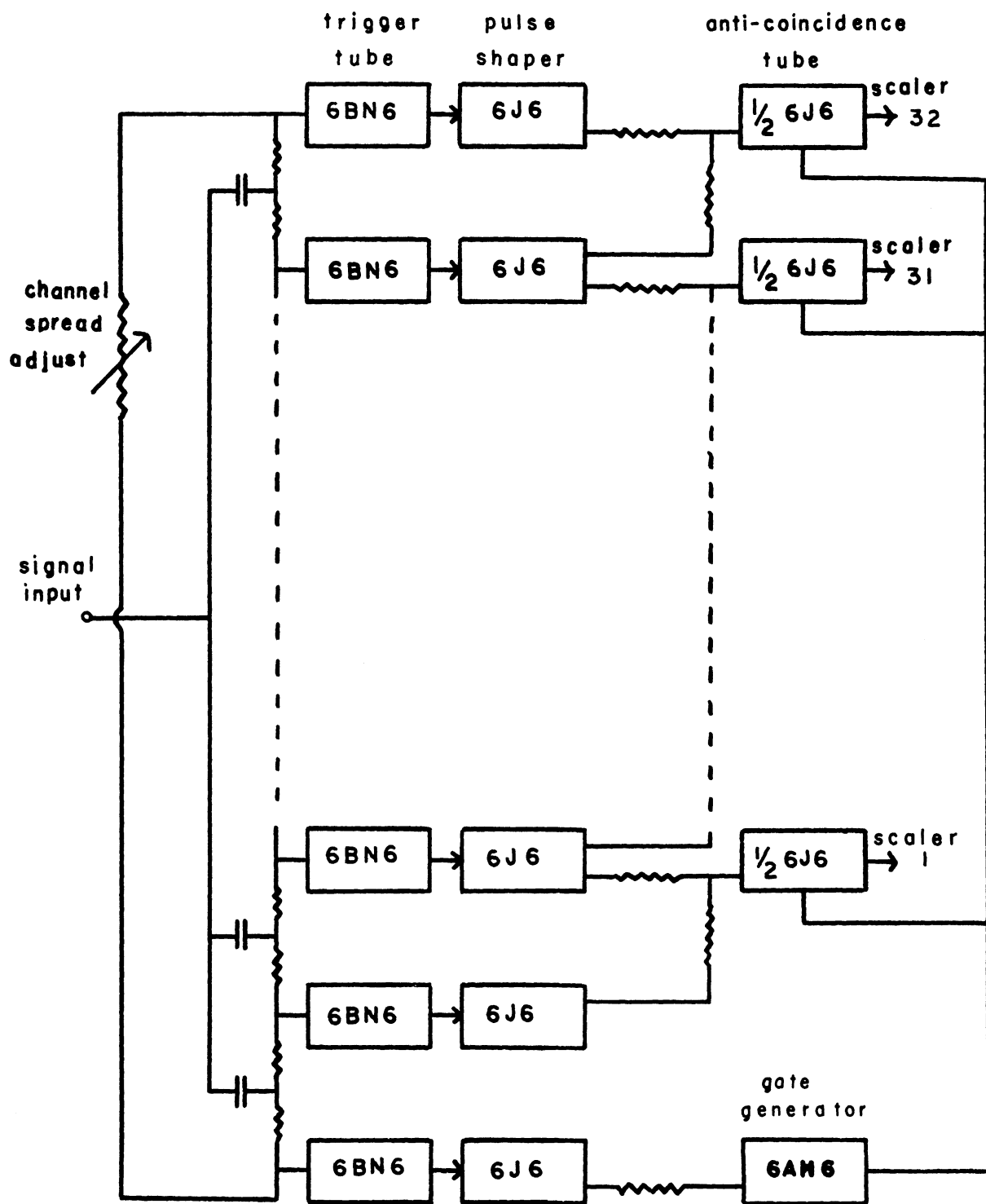


Figure 5. The Block Diagram of the Pulse Height Analyzer

Multi-Channel Differential Analyzer--A multi-channel differential analyzer is a device for taking pulse height distribution. At present stage of nuclear spectroscopy, the design of a fast multi-channel analyzer is of considerable interest. A block diagram of the analyzer used in this study is shown in Figure 5.

Discrimination is obtained by biasing the trigger tubes beyond cutoff at successively lower but equally spaced voltages. Each channel takes two trigger circuits for its lower and higher boundaries; its width is given by the bias difference of the two trigger levels. For statistical accuracy, the boundaries must be maintained as stable as possible. The above-shown analyzer has a channel width of 3 volts, and therefore a 2% width stability requires that the boundary should be stable within 0.1 volt. The gated-beam tube 6BN6 provides a sharp trigger level and can be driven to over 100 volts positive without overloading. Width stability is improved by connecting all filaments of the 6BN6's in series to avoid any relative boundary drift. In general this type of tube is quite satisfactory for its use as trigger tube. But it has at least one drawback, that is, its cutoff voltage shows notable changes after being in use for periods of several days. The input signal is lengthened to a duration of 4 microseconds for proper triggering of the univibrators. This also fixes the resolving time of the analyzer. The negative signal from the plate of the trigger tube actuate a sudden change of state in the univibrator. The right-hand side tube which is normally conducting, is now cutoff, and the left-hand side tube is fired. The univibrator returns to its normal state after a certain recovery time dominated by the

duration of the triggering signal. A recovery time of 4 microseconds can be chosen for all the univibrators by adjusting the trimmer condenser. The negative and positive pulses from the plates are 30 and 20 volts respectively. The negative pulse of one trigger level is mixed with the positive pulse of the next higher level through resistors leading to the grid of an anticoincidence tube. If the upper level is not triggered, no cancellation of pulses is possible, the anticoincidence tube of the lower level fires and a count is recorded by the following scaler. Since the input signal has a finite rise time, it appears later at the higher level than at the lower level. A gate signal is thus needed to insure that no count is registered when there is actually an anticoincidence. The gate signal is coupled to the cathodes of the anticoincidence tubes and can be chosen of length 2 to 3 microseconds. The time relationship is such that no registering pulse is formed until 2 to 3 microseconds after the arrival of the input signal.

A multiple position switch provides three different bias settings for the discriminator. When the switch is in position 2 or 3, the bias voltages relative to ground are 152, 149,.....42 volts or 265, 262,.....155 volts instead of 39, 36,.....-61 volts as in position 1. Hence ninety channels are available, if measurements are taken at three different bias settings.

The equality of channel width is best achieved with the use of a sliding pulser. By changing the plate resistors of the 6BN6's or the tubes themselves enough bias variations can be obtained for boundary adjustment.

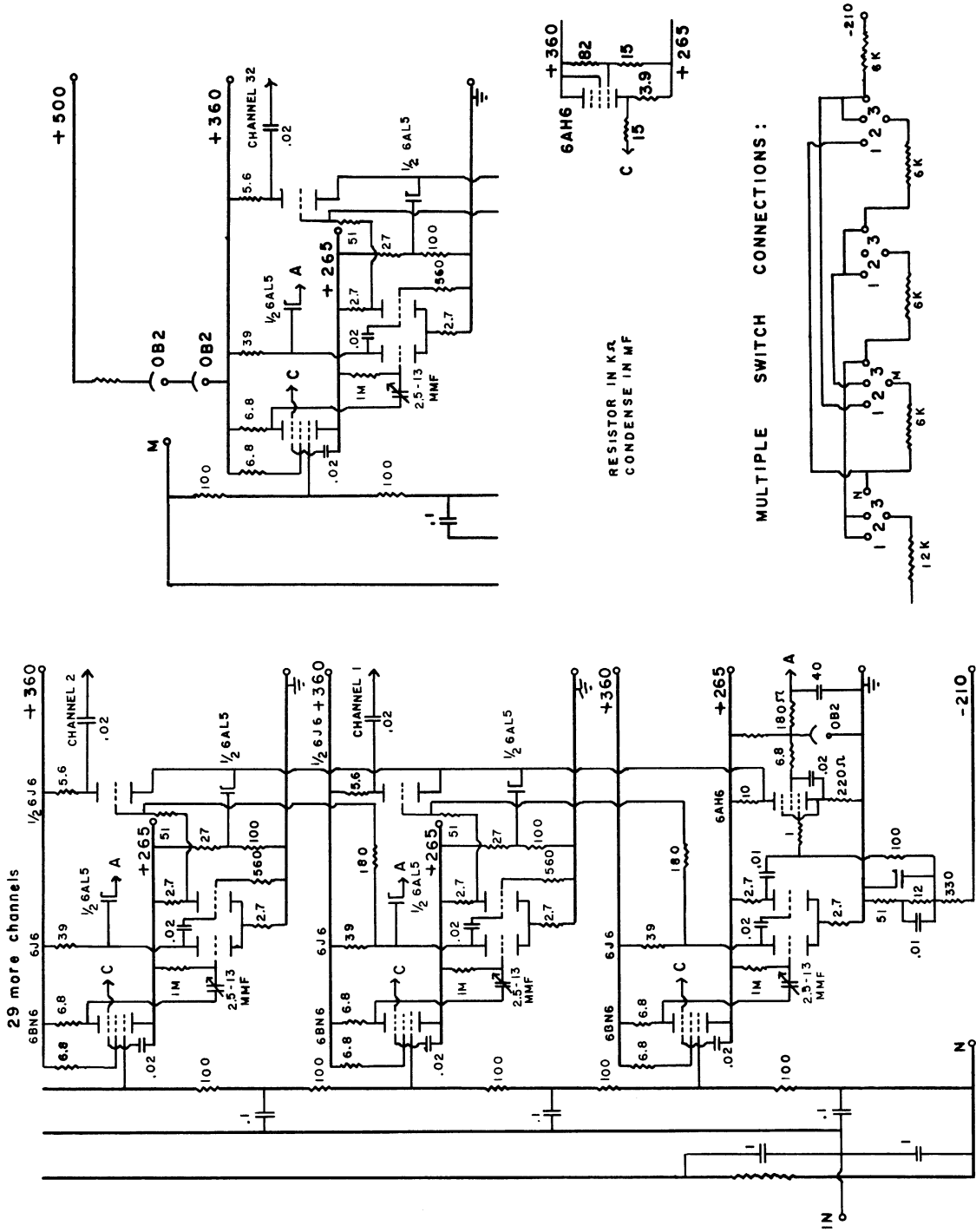


Figure 6. The Pulse Height Analyzer Circuit

Decade Scaler--The construction of the scalers is greatly facilitated by the use of Philips EIT tubes, which reduce the number of tubes and other components in the circuit. Each scaler contains a univibrator, a scale-of-four and five stages of EIT tubes. The scale-of-four is necessary because the EIT tube has a recovery time of about ten microseconds. Zero-setting of the EIT tube is accomplished by means of a coupling condenser. The value of this condenser at the first stage must be kept small, since it determines to a large extent the recovery time of the tube. The electron beam inside the tube has ten stable positions. A pulse of proper shape and magnitude applied to the right deflection plate will move the beam from one position to the next. The usual troubles encountered in the operation are "skipping", resetting not to zero, and "sticking". These can often be overcome by changing the values of the anode resistor, the coupling condenser, and the control grid voltage. A circuit diagram of the scaler is shown in Figure 7.

The oscilloscope used is a Tektronix type 531. The +265 and -210 volts, +360 volts and +1050 volts power supplies are of the usual electronically regulated type. All 110 A. C. input voltages were also regulated.

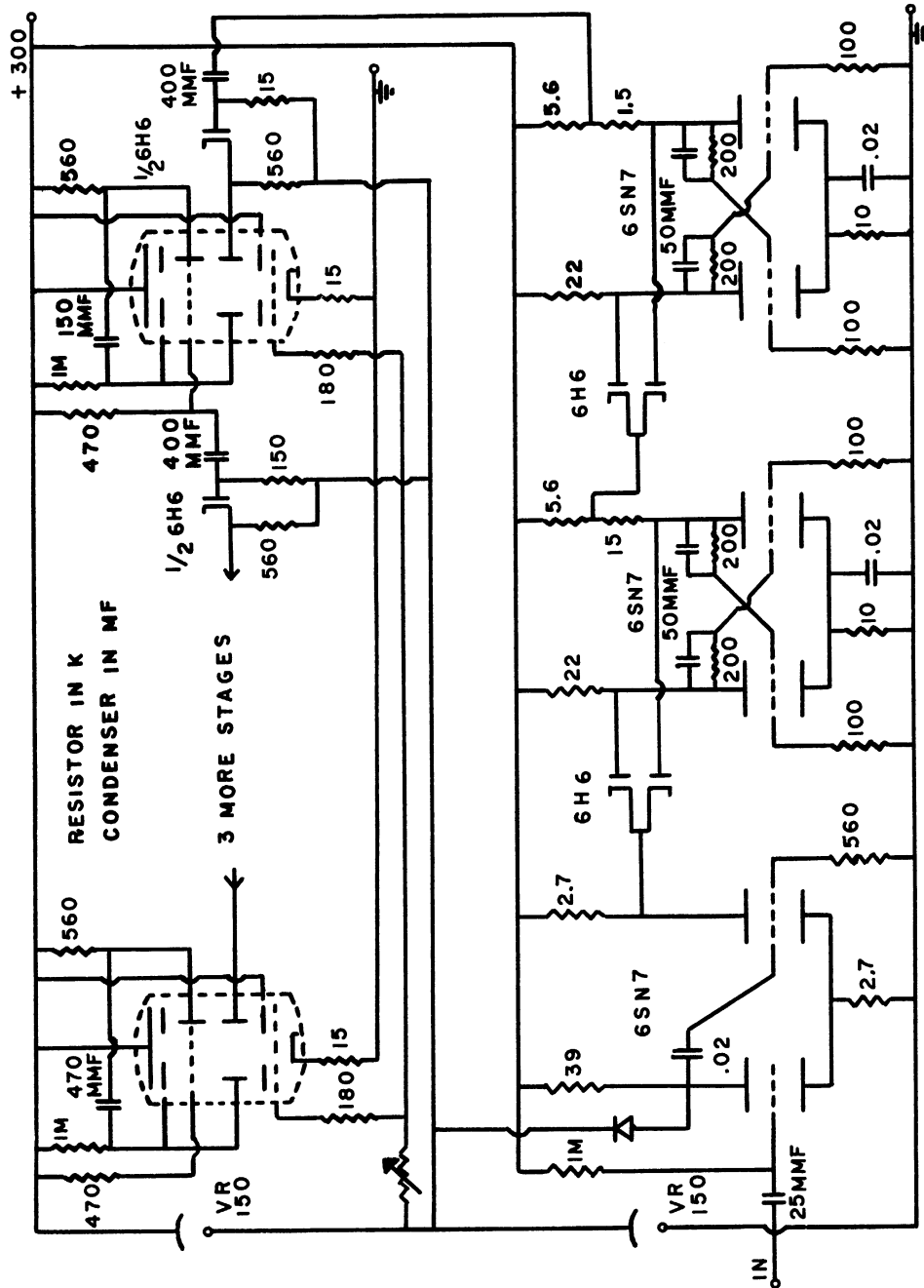


Figure 7. The Scaler Circuit

CHAPTER III

RESULTS

The study of nuclear structure is still at its early stage. Its difficulty is partly due to the mathematical complexity involved in the application of quantum mechanics to a many-body system. Besides, we know little about the nature of the forces which hold together the nucleons. One of the goals of meson theory is the understanding of nuclear forces. In view of our lack of any satisfactory meson theory, we can at best assume a model for the nucleus and explain the nuclear phenomena on the basis of the model.

In the present study we are concerned with the energies and relative intensities of the gamma-rays emitted by artificial radioactive nuclei and the coincidence relations among them. The production of radioactivities were accomplished by means of three different methods: slow neutron capture, deuteron bombardment and bremsstrahlung irradiation. One possibility is that the bombarded nucleus is left in an isomeric state and it then returns to the ground state by emitting one or more gamma-rays. Another possibility is that the resulting nucleus is unstable against beta-decay and gamma rays are emitted following beta emission. In either case the measurement of the energies and intensity ratios of the gamma-rays yields information concerning energy levels of the gamma-emitting nucleus. When an energy level diagram is definitely established, other features of the levels, such as, spin and parity can be found by angular correlation or internal conversion measurements.

An attempt will also be made to interpret the observed results in terms of shell model or collective model.

Cu⁶² and C¹¹ (36).

Due to the presence of scattering peaks the interpretation of scintillation spectra is not always straightforward. These peaks arise as a result of Compton scatterings taking place in the surroundings of the crystal or the edges of the crystal and resemble the photopeaks of gamma rays. The first three examples may illustrate this point.

A copper cylinder of 1/4 inch in diameter and one inch long was used to produce the 9.8 minute activity of Cu by (γ , n) reaction. The 0.7 mev peak in the summed spectrum (figure 9) can be explained if one assumes that a 0.2 mev gamma ray follows the positron emission. If this is the case, one expects to find a sum peak at 1.22 mev corresponding to a coincidence of this gamma ray and a pair of annihilation photons. But such a peak was not found. For further study the spectra of C¹¹, which is known to be a pure positron emitter, were measured. The source was a lucite cylinder of one inch length and 1/4 inch diameter. The same procedures in the measurement of Cu⁶² were also followed here, and the spectra (figures 10 and 11) were normalized for easy comparison. The main difference between the spectra of the two isotopes seems to be the presence of a 0.7 mev peak in one but not in the other. However, a similar peak arises in C¹¹ spectrum, if the source (of smaller diameter) is enclosed in a 1/16 inch thick copper container (figure 12). The false peak can thus be ascribed to Compton scattering in copper.

Reid and Wright have shown that there is no gamma ray in the range 0.1 - 1.2 mev in the decay of Cu⁶². Our search for gamma rays

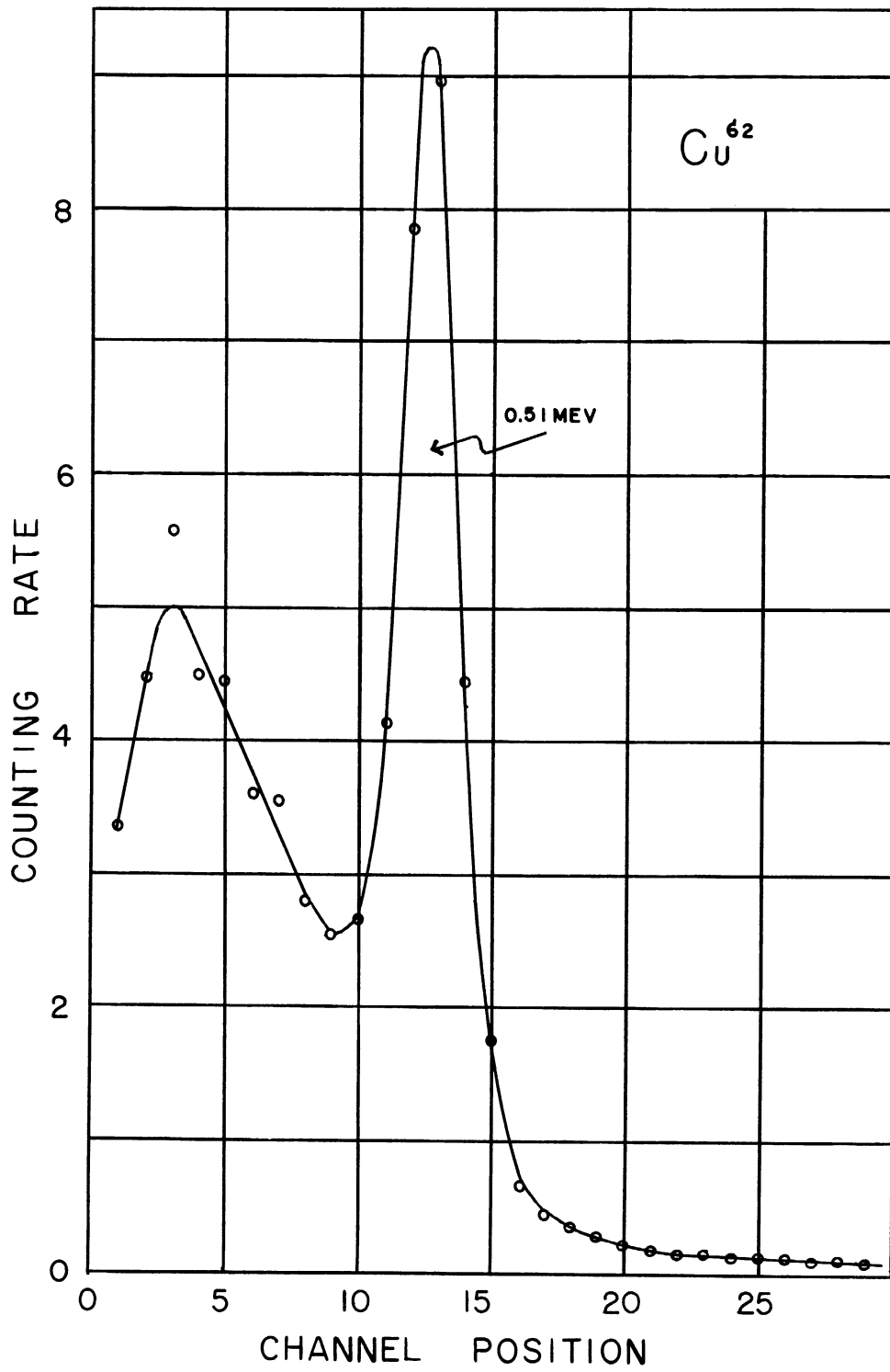


Figure 8. The Normal Gamma Spectrum of Cu⁶²

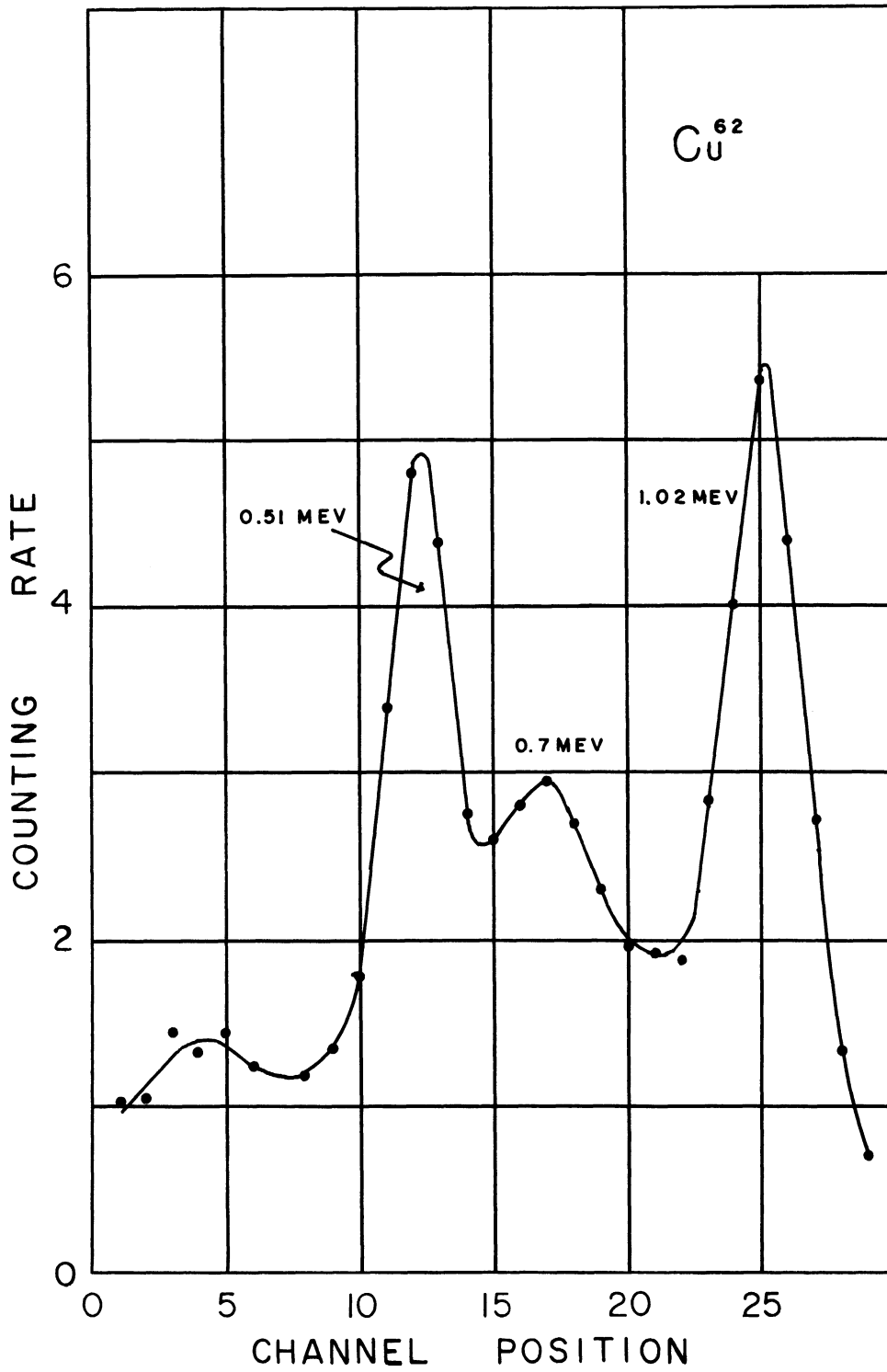


Figure 9. The Sum Gamma Spectrum of Cu⁶²

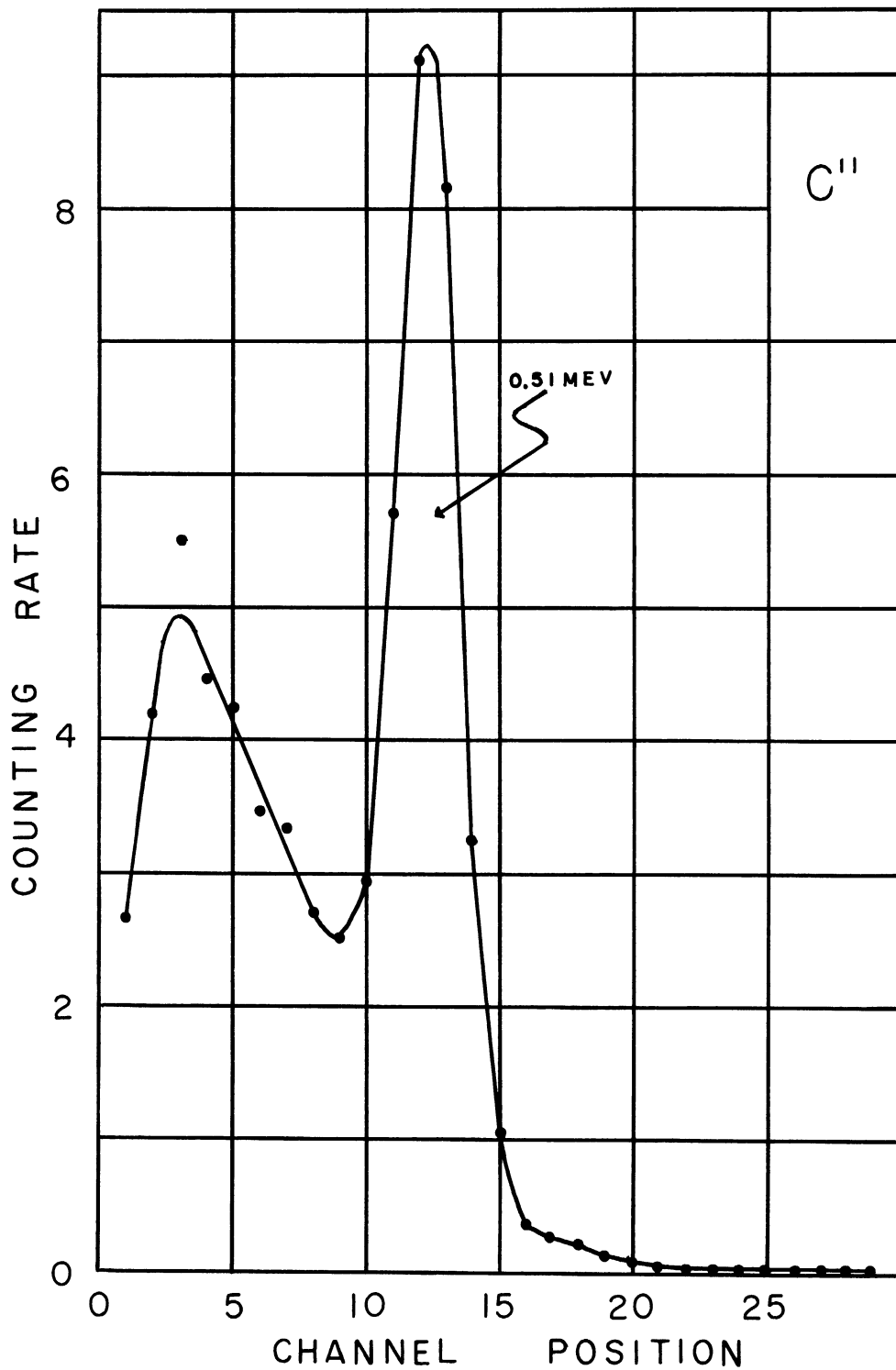


Figure 10. The Normal Gamma Spectrum of C¹¹

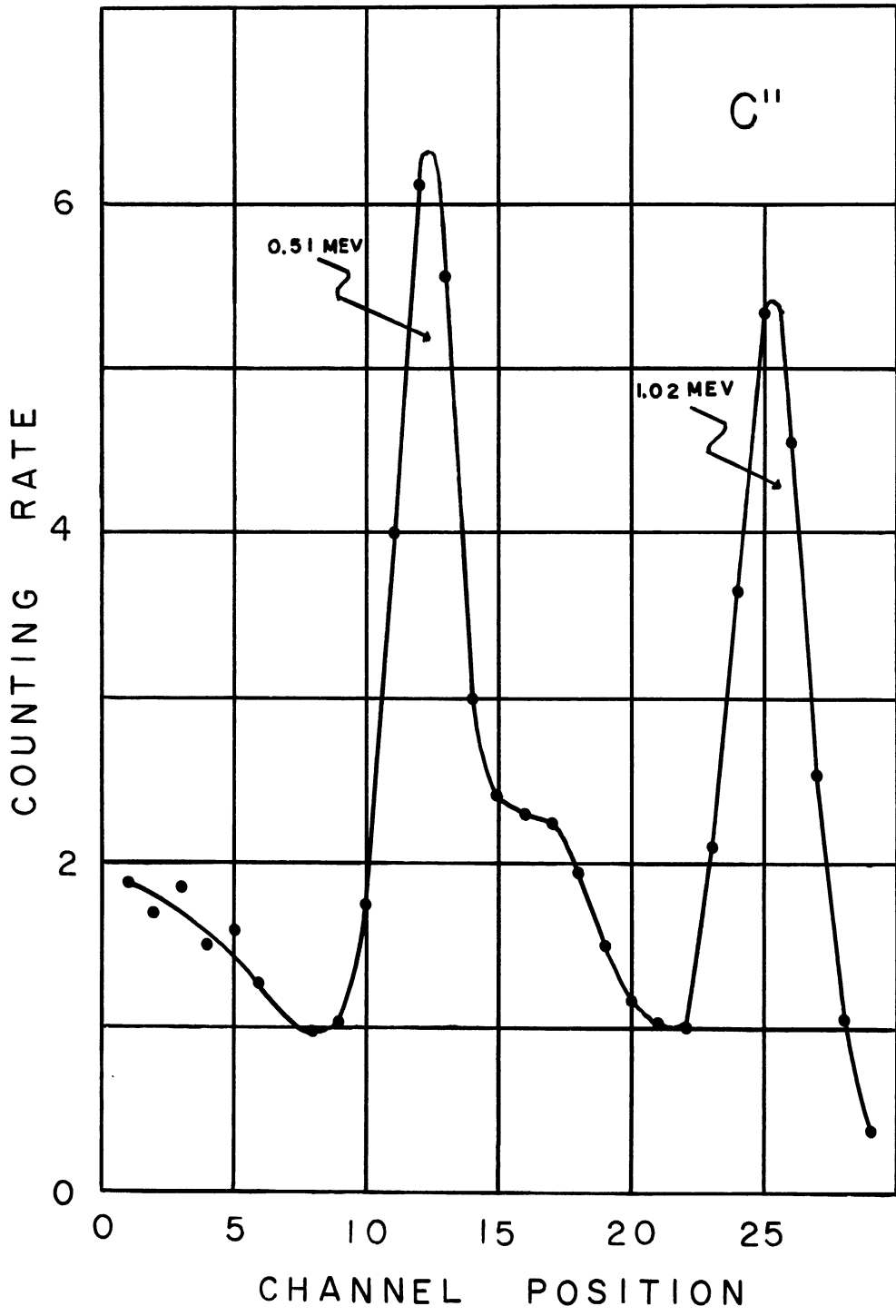


Figure 11. The Sum Gamma Spectrum of C¹¹

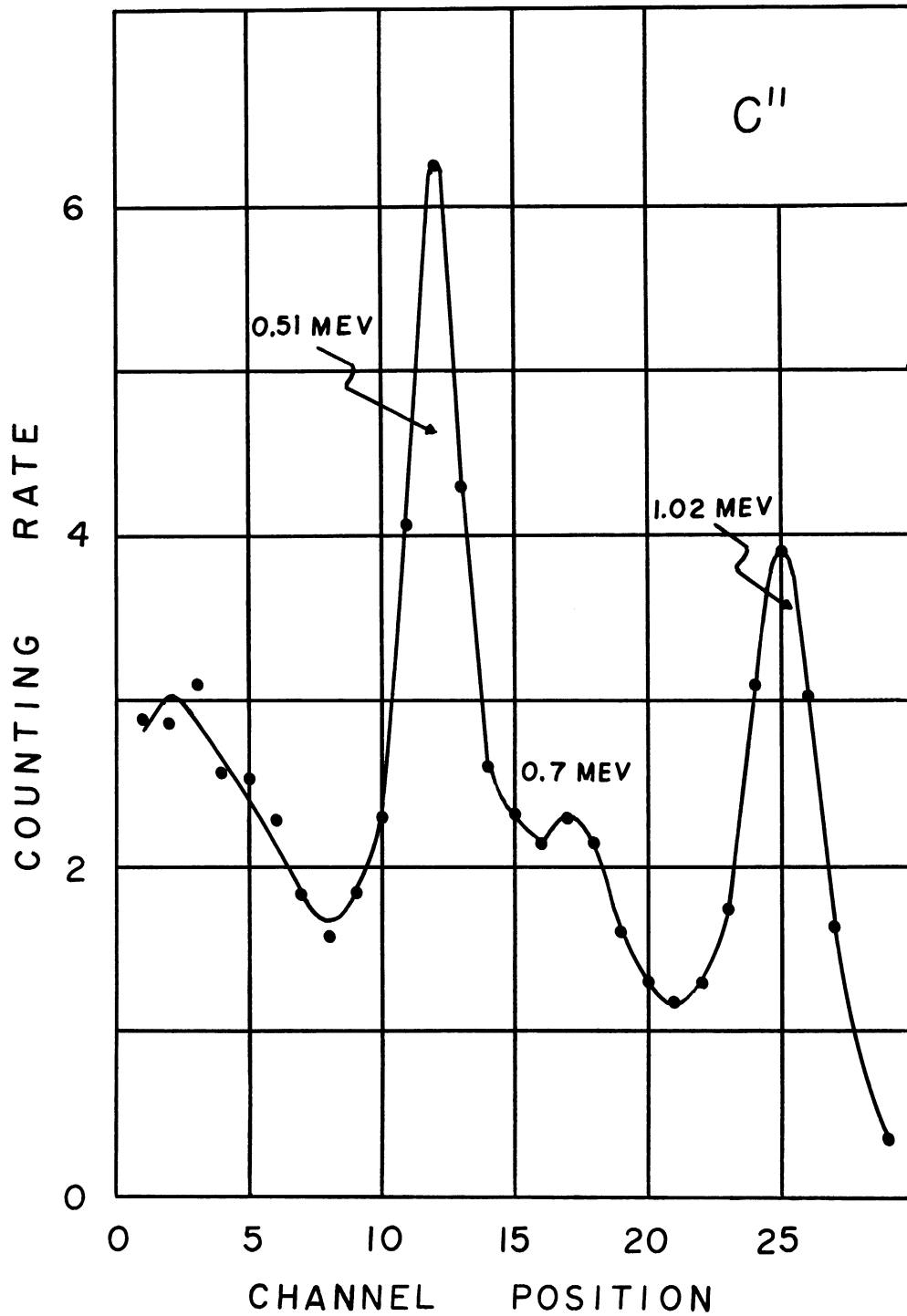


Figure 12. The Sum Gamma Spectrum of C^{11} with the Source Enclosed in a Copper Container

beyond 1.22 mev obtains negative results. It can therefore be concluded that Cu^{62} decays to the ground state of Ni^{62} solely by positron emission.

Co^{57} (7,26,15)

Cork and collaborators have reported that in the decay of this isotope six gamma rays are present with energies 14.6, 29, 99.8, 122.8, 137.4, and 700 kev. By means of coulomb excitation Temmer and Heydenburg have found an excited level at 137 kev in Fe^{57} . Delayed coincidence measurements showed that this level decays either to the ground level or to a metastable level at 14 kev and thence to the ground level.

The source used in our work was obtained from Oak Ridge National Laboratory. It was prepared by proton bombardment of nickel. The summed spectrum shows a peak at 225 kev. When the source is moved to a distance of 6 inches from the crystal, this peak vanished. It is further noted that in the normal spectrum (figure 13) a peak exists at about 95 kev and its intensity is reduced when the source is inside the crystal. One is tempted to say that an excited level exists at 225 kev in Fe^{57} . However, the sum peak is too weak to account for the large intensity reduction of the 95 kev peak. From energy considerations the 95 kev peak may correspond to the Compton scattering of the 123 and 137 kev gamma rays. Gamma-gamma coincidence measurements also failed to show any cascade relation between this and the latter two gamma rays. It is then concluded that the 225 kev peak represents the sum of the 123 or 137 gamma rays and the backscattered photons.

Neither the 29 kev gamma ray nor positron annihilation photons were found. The 700 kev gamma ray is weak compared to other gamma rays

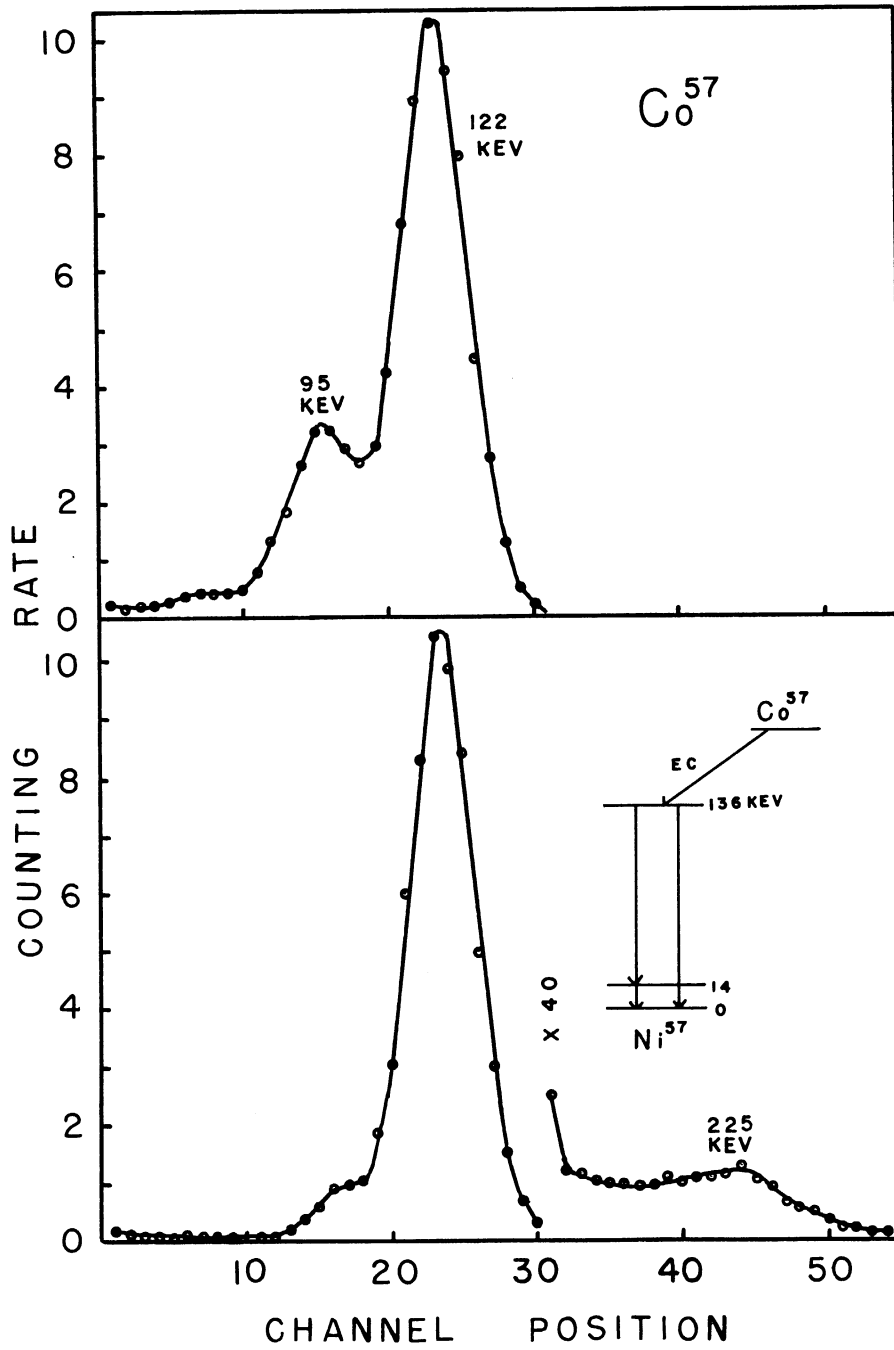


Figure 13. The Normal and Sum Gamma Spectra of Co^{57}

observed; it does not seem to be affected by summing effect. It might be from some impurity in the source. These results confirm the decay scheme proposed by other authors.

Rb⁸⁶ (8,24,34)

In 1954 and 1955 it was reported that besides the 1.08 mev gamma ray and 0.71 and 1.8 mev beta particles, other gamma ray and beta particle are present in the decay of this isotope. Our sample was obtained from Oak Ridge National Laboratory. In the normal and summed spectra shown in Figures 14 and 15 it is impossible to identify any other gamma ray besides the one at 1.08 mev due to the strong bremsstrahlung of the beta particles.

On the basis of the shell model the ground state configurations can be given as below:

$_{38}^{86}\text{Sr}_{48}$: protons: 28 in closed shell,
4 in 3p 3/2
6 in 4f 5/2

neutrons: 28 in closed shell
4 in 3p 3/2
6 in 4f 5/2
2 in 3p 1/2
8 in 5g 9/2

$_{37}^{86}\text{Rb}_{49}$: protons: 28 in closed shell
4 in 3p 3/2
5 in 4f 5/2

neutrons: 28 in closed shell
4 in 3p 3/2
6 in 4f 5/2
2 in 3p 1/2
9 in 5g 9/2

The ground state spin for Sr⁸⁶ is expected to be 0 +. Nordheim's rule predicts a ground state spin of 2 for Rb⁸⁶. (Nordheim's rule

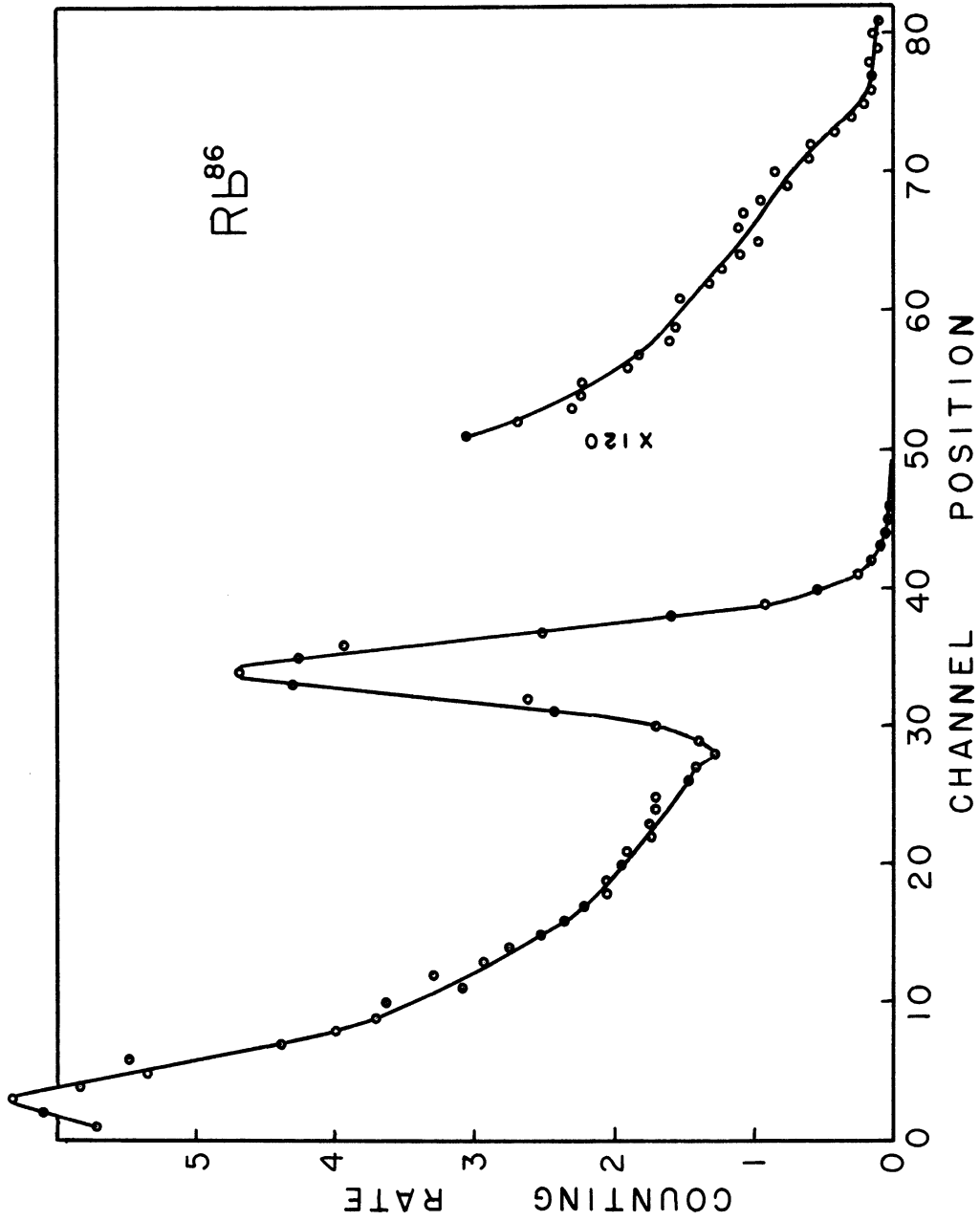


Figure 14. The Normal Gamma Spectrum of Rb^{86}

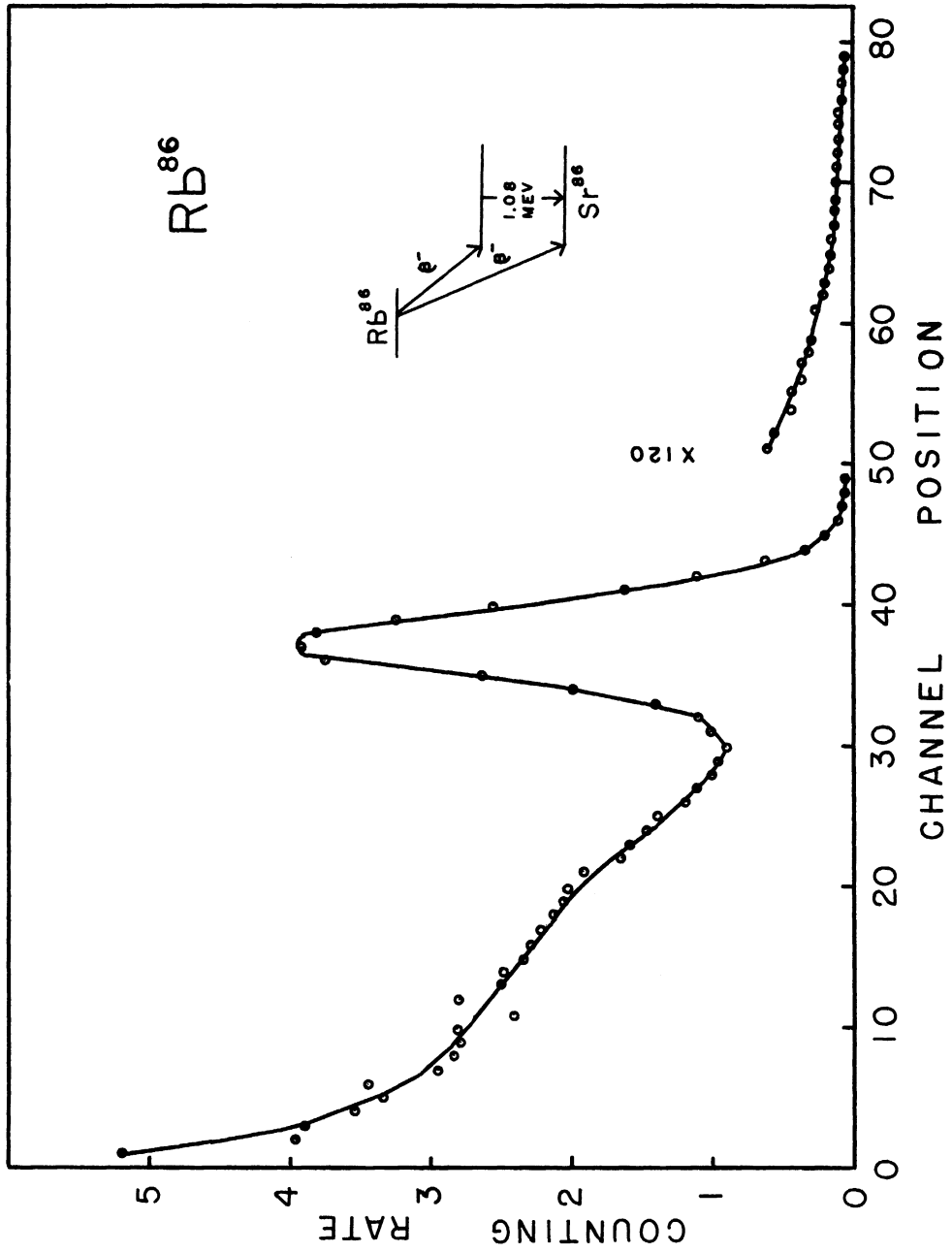


Figure 15. The Sum Gamma Spectrum of Rb^{86}

states that if the odd proton and neutron groups have different relative orientation of intrinsic spin and orbital angular momentum then their resultant spins subtract, otherwise they add to a value greater than the smallest possible one. This rule fits the observed spins of many odd-odd nuclei.).

The ft values for the ground to ground, and ground to the excited state transitions from Rb to Sr are 8.5 and 7.8, respectively, according to Pohn et al. The selection rule for once forbidden beta transition requires that the ground state parity of Rb be odd, and the parity of the excited state of Sr be even.

In terms of single particle excitation, the ground to ground beta transition is accomplished by transforming a $5g\ 9/2$ neutron into a $4f\ 5/2$ proton. If this neutron is changed into a proton in some other levels, $3p\ 1/2$ or $5g\ 9/2$ a number of final states of various spins would be allowed by selection rules and it would be difficult to explain the predominance of just one gamma transition in Rb^{86} . (By addition of angular momentum, a $f\ 5/2$ proton and a $p\ 1/2$ proton can give levels with total angular momentum 2 and 3. Similarly, a $f\ 5/2$ proton and a $g\ 9/2$ proton can give levels with total angular momentum 2, 3, 4, 5, 6, and 7. Five of these levels; namely, $(f\ 5/2, p\ 1/2)_{2,3}$ and $(f\ 5/2, g\ 9/2)_{2,3,4}$ are allowed by selection rules.) On the other hand, if the excited level is interpreted as a vibrational level, this would be the only possible vibrational level on energy consideration and a consistent assignment of spin 2 + can also be made.

Cr⁵¹ (4)

Using a NaI scintillator, Bisi and Germagnoli found a new line in the decay of Cr⁵¹ with energy at 624 kev. They did not exclude the possibility of a weak transition from the proposed level at 624 kev to the one at 324 kev. The sample was supplied by Oak Ridge National Laboratory. The normal spectrum (figure 16) was taken with the source at a distance 6 1/2 inches from the crystal. In addition to the strong line at 325 kev, a weak one does exist at 630 kev superposed upon a continuous distribution. The height ratio of the two peaks remain constant over a period of 40 days, indicating that they probably belong to the same activity. Several summed spectra were obtained with different source strengths, the height of the weak line relative to the strong one decreases with decreasing source strengths and the spectrum finally becomes essentially identical with the normal spectrum. This indicates that coincidences occurred between gamma photons and back scattered photons. We therefore concluded that there is no transition from the 624 kev level to the 325 kev level.

The assignment of shell model configurations is straightforward.

${}_{24}\text{Cr}^{51}$:	protons:	20 in closed shell 4 in 4f 7/2
	neutrons:	20 in closed shell 7 in 4f 7/2
${}_{23}\text{V}^{51}$:	protons:	20 in closed shell 3 in 4f 7/2
	neutrons:	20 in closed shell 8 in 4f 7/2

We thus expect the ground level character for both isotopes to be 7/2-.

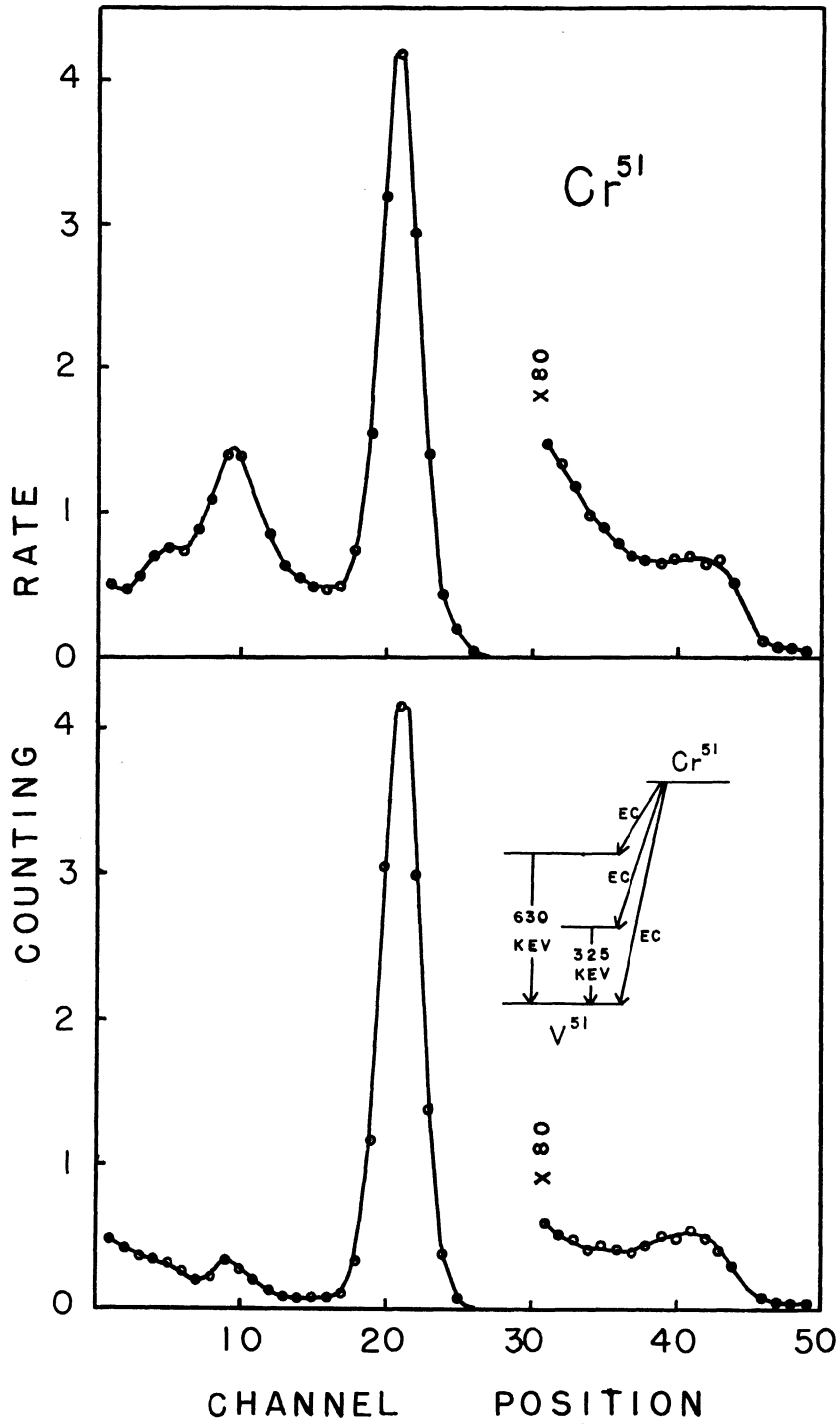


Figure 16. The Normal and Sum Gamma Spectra of Cr^{51}

The beta transition from the ground state of Cr^{51} to the 624 keV level in V^{51} is most likely once forbidden. The 624 keV level must therefore have even parity. Between proton numbers 20 and 50, the only level which can give rise to an even parity is $5g\ 9/2$. This also agrees with the expectation that for protons an orbit of higher orbital momentum is favored. As for the 324 keV level, it should have odd parity as required by the beta selection rules. Together with l -selection rule we are left with the only possible level $4f\ 5/2$. This assignment seems to be consistent with our data.

Ta^{182m} (46,1)

In 1950 Wilkinson, using aluminum absorption techniques, found that conversion electrons, beta particles and gamma rays were present in the decay of Ta^{182m} in the ratios of $\sim 0.2 : \sim 0.05 : 1$. In 1951 Sunyar determined the conversion coefficient for the gamma ray of energy 180 keV from the ratio of the K x-rays intensity to the gamma intensity by means of a scintillation counter. α_K was found to be 0.8 ± 0.3 on the assumption that only one gamma ray was involved in the decay.

A thin foil of tantalum metal was bombarded for one-half hour with 7.8 MeV deuterons. Spectra was taken immediately after bombardment. The normal spectrum, Figure 17, consisted of intense lines at 70 keV and 170 keV and weak lines at 340 keV and 510 keV. The decay of each of these lines was followed and the three lowest energy lines were found to have identical half-lives of 16.5 minutes. The 510 keV line has a 10-minute half-life and does not appear to be associated with the other lines. Its origin is not now known.

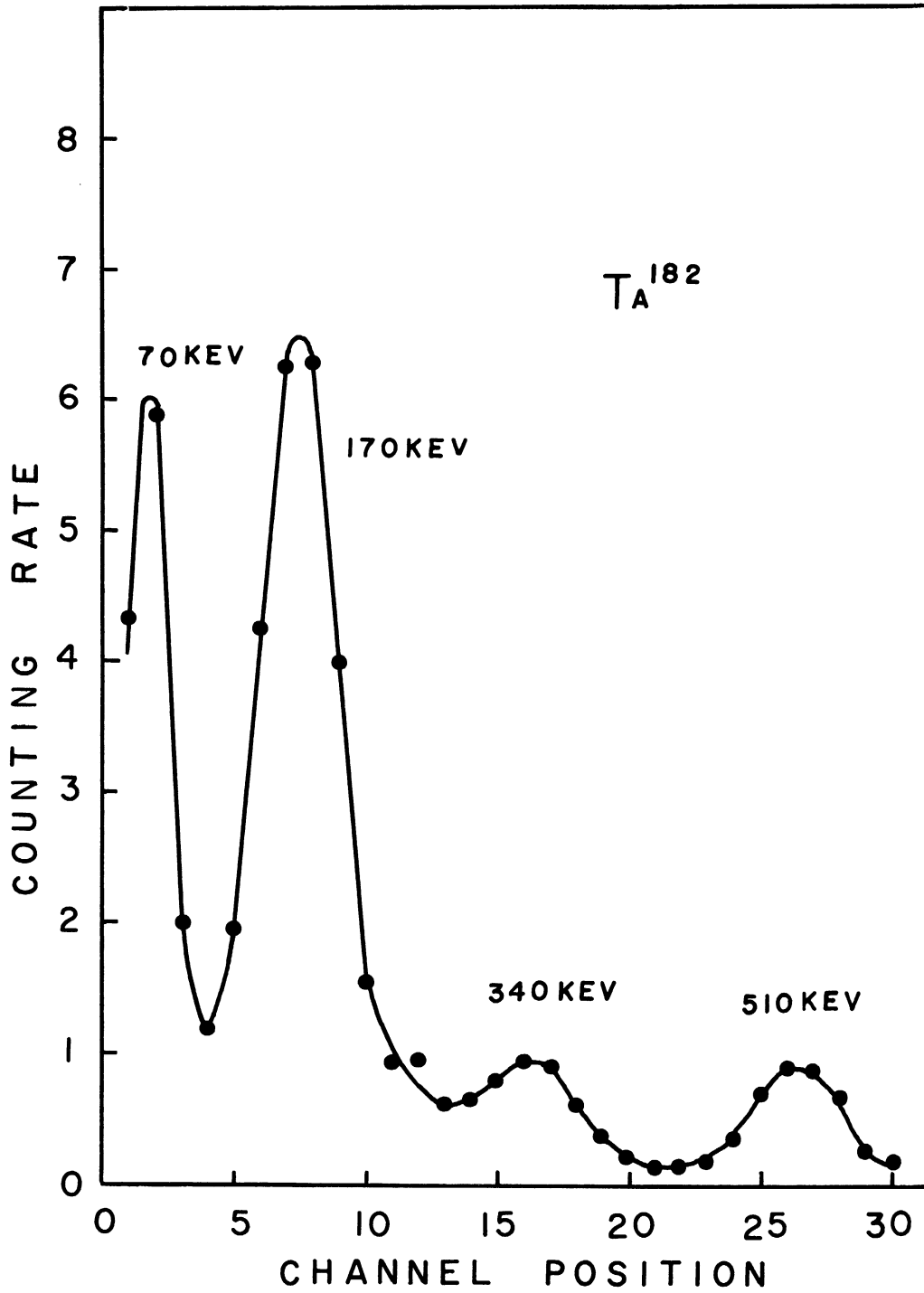


Figure 17. The Normal Spectrum of Ta^{182m}

The sum spectrum, Figure 18, shows several interesting features. First, the line at 170 kev is greatly depleted relative to the 70 kev line. Second, the line at 340 kev is somewhat strengthened. Third, a new line appears in the region of 230 kev.

The 70 kev line is interpreted as being the K x-ray line arising from the electron capture in the decay of the metastable state. The new line in the sum spectrum at 230 kev is due to the summing of the 70 kev x-ray line with another unconverted gamma ray of about 170 kev energy. The increased intensity of the 340 kev peak arises from the summing of the two gamma rays in the region of 170 kev each. A decay scheme consistent with these observations is shown in Figure 18. Similar results were obtained by P. Axel and A. W. Sunyar, but the details of their measurements have not been published.

Cl³⁴ (43,16,31)

A 33-minute activity was produced in chlorine when bombarded by the x-rays from an 80 mev synchrotron beam. The normal spectrum, Figure 19, shows an intense line at 0.145 mev with weaker gamma lines at 1.16 and 2.10 mev. A peak at 0.51 mev arises from the positron annihilation. The chief feature of the sum spectrum, Figure 20, is the lack of summing by the strong 0.145 mev line. Peaks were found which arise from the summing of the annihilation radiation with the 1.16 mev and 2.10 mev lines as well as a line at 3.2 mev arising from the summing of the 1.16 mev and 2.10 mev gamma rays. These data are consistent with the decay scheme proposed by Strahelin and Preiswerk. Based on the experimental results on beta transitions and angular

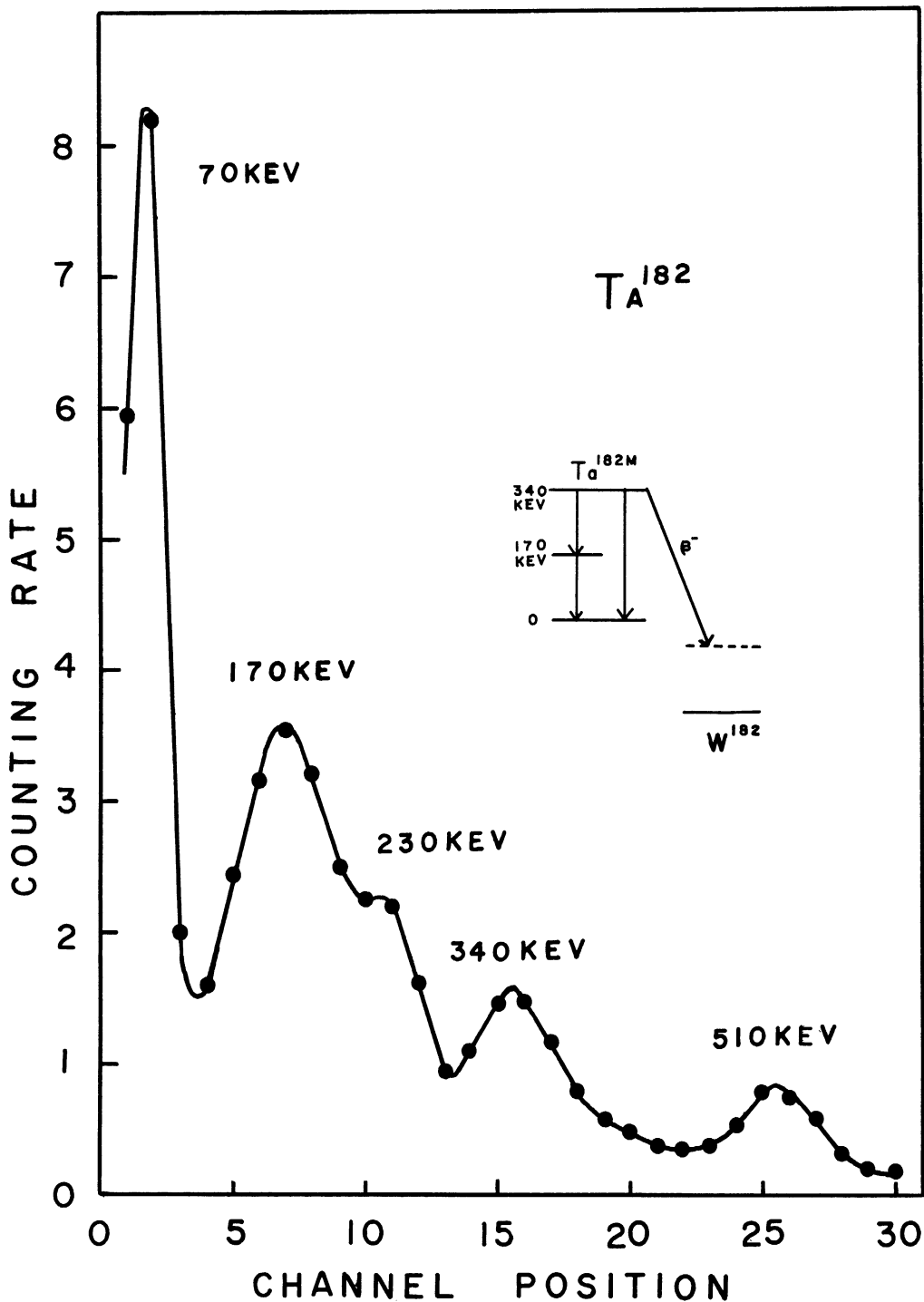


Figure 18. The Sum Gamma Spectrum of Ta^{182m}

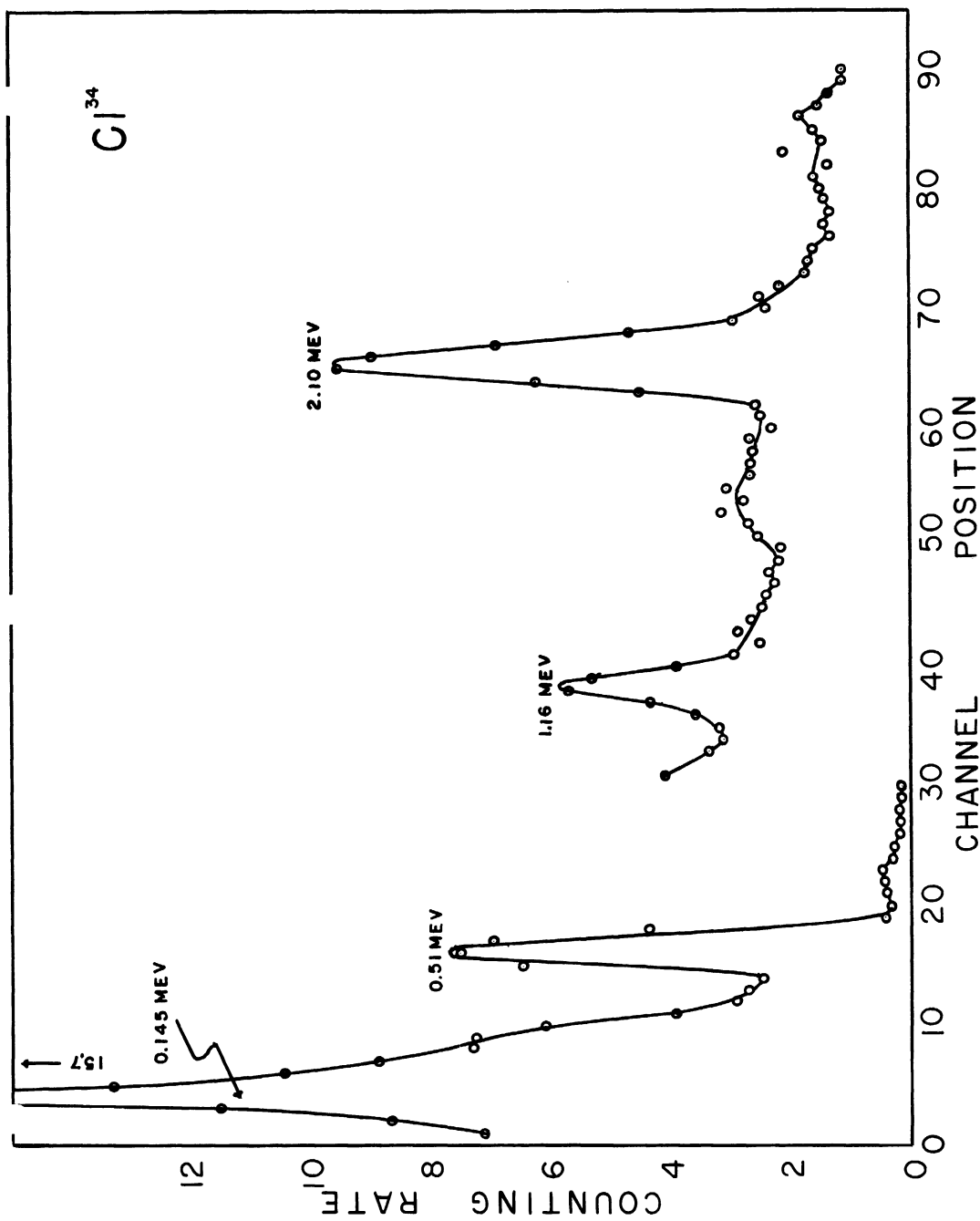


Figure 19. The Normal Gamma Spectrum of Cl^{34}

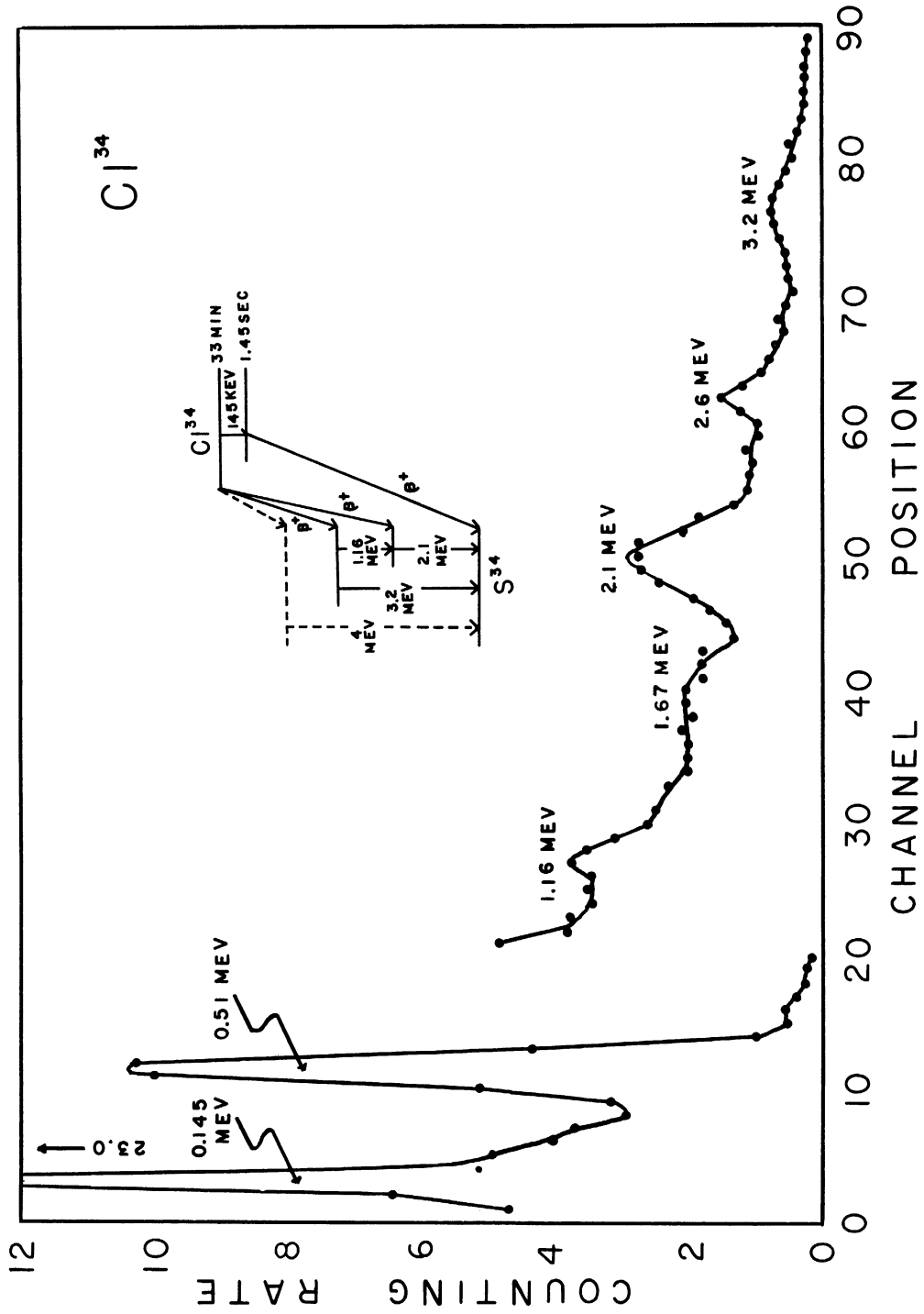


Figure 20. The Sum Gamma Spectrum of Cl^{34}

correlation, the values for spin 0, 2, 2, and all even parity can be assigned to the ground state and the two excited states. A shell model interpretation of the levels was made by Morinaga and Bleuler.

Dy¹⁶⁵ (23,18,14)

By means of photographic internal conversion electron spectrometers and a scintillation coincidence spectrometer, Jordon and others were able to propose a decay scheme for Dy^{165m} (1.2 min.) and Dy¹⁶⁵ (2.3 hr.). We have studied the 2.3 hour activity by our method. The source was prepared by slow neutron bombardment of dysprosium oxide. The spectra are shown in Figures 21 and 22. From the normal spectrum it is seen that six gamma rays with energies 0.094, 0.279, 0.361, 0.634, 0.710 and 1.02 mev are present. The sum spectrum shows that the 0.094 mev line is not summed and therefore must correspond to ground state transition. If we take the 0.094 mev line as a reference and compare the heights of the other lines, we observe that the intensity of the 1.02 mev line is strengthened while the other four lines are weakened. It can be concluded that the 0.279 and 0.710 mev as well as the 0.361 and 0.634 mev gamma rays are coincident. These results are consistent with the decay scheme proposed by Jordan, Cork, and Burson.

By means of coulomb excitation Heydenburg and Temmer established rotational levels in Ho¹⁶⁵ at 94 kev and 208 kev. The measured spin of Ho¹⁶⁵ is 7/2. Shell model gives the following configuration for the ground state of Ho¹⁶⁵.

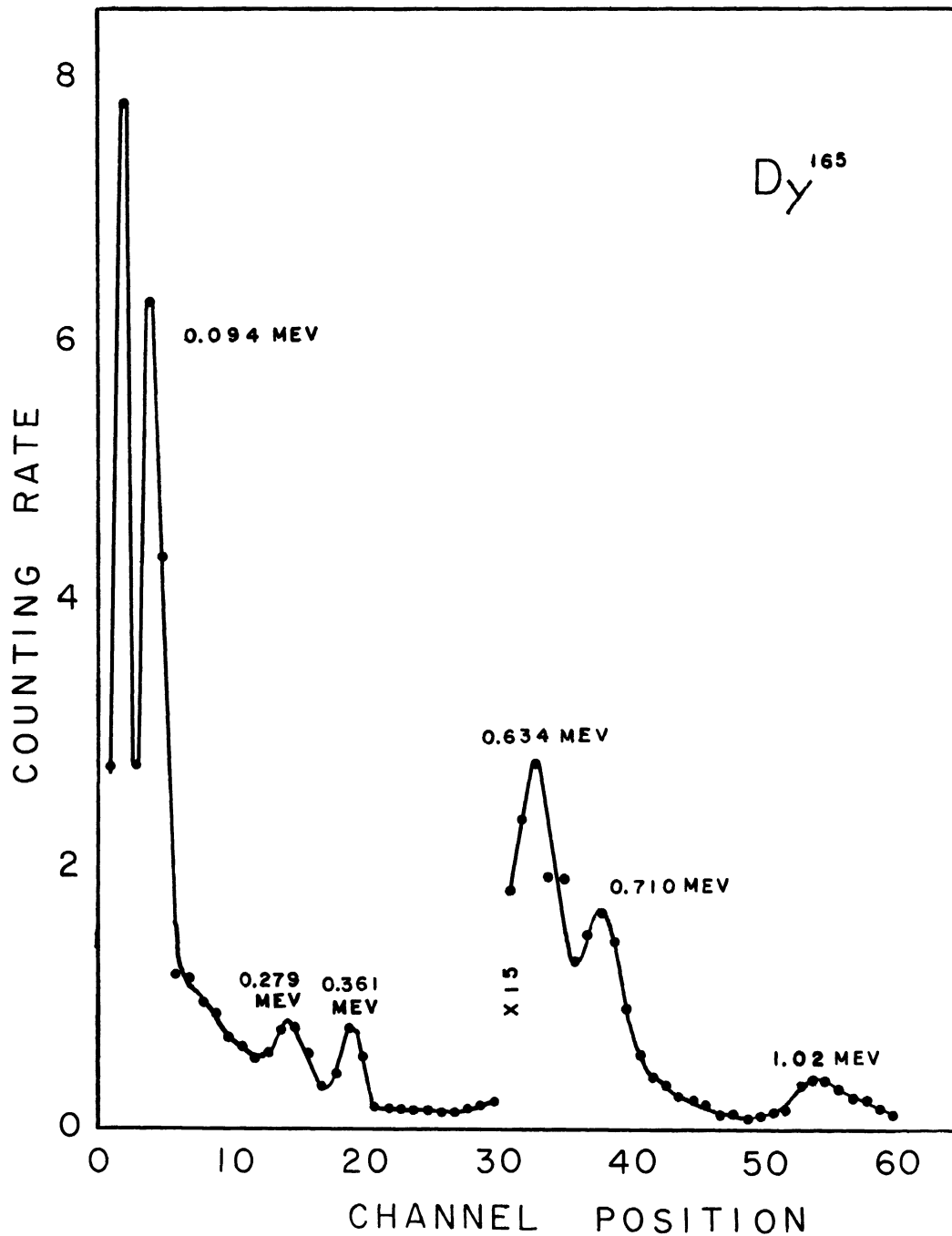


Figure 21. The Normal Gamma Spectrum of Dy^{165}

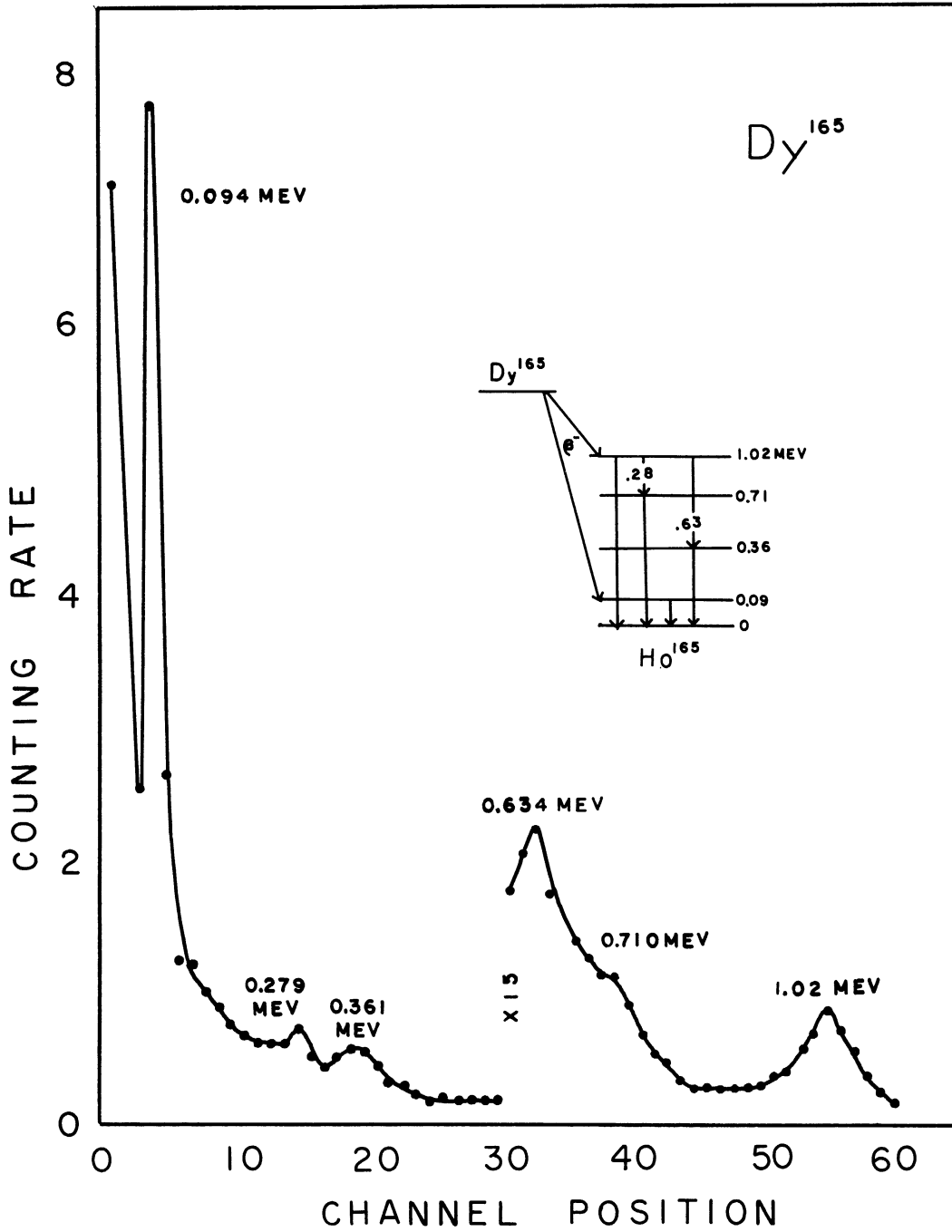


Figure 22. The Sum Gamma Spectrum of Dy^{165}

protons: 50 in closed shell
7 in 5g 7/2
6 in 4d 5/2
4 in 6h 11/2

neutrons: 82 in closed shells
6 in 5f 7/2
10 in 6h 9/2

It follows that the ground state of Ho¹⁶⁵ is even. The character of the level at 94 kev is then expected to be 9/2 +.

The log ft values of beta transitions from Dy¹⁶⁵ to Ho¹⁶⁵ were reported by Goldhaber and Hill.

<u>energy</u>	<u>log ft</u>	
1.25 mev	6.15	once forbidden
0.88 "	6.52	once forbidden
0.42 "	5.44	allowed

The ground state configuration for Dy¹⁶⁵ is possibly as follows.

protons: 50 in closed shells
6 in 5g 7/2
6 in 4d 5/2
4 in 6h 11/2

neutrons: 82 in closed shells
7 in 5f 7/2
10 in 6h 9/2

The absence of beta transitions to the second and fourth excited states may be an indication that the configurations of these levels are relatively pure. An assignment of d 3/2 to the second excited level seems to be the only one consistent with this picture of single particle excitation. The weak transition from the fourth excited level to the ground level favors the assignment of h 11/2 to the former. The 1.02 mev level may have mixed configuration with a spin 7/2.

Tc⁹⁶ (29,30,11,44)

Medicus and others measured the conversion electrons with a magnetic lens spectrometer. Five gamma rays were found at 312, 771, 806, 842, and 1119 keV with intensity ratios 0.0052: 1.00: 0.82: 1.00: 0.17. Gamma-gamma coincidence measurements with both Bi and brass cathode counters revealed that the 771, 806, and 842 keV gammas are in three-fold cascade. From coincidence rate and intensity considerations they concluded that the 1119 keV, 842, and 771 keV gammas are also in three-fold cascade. In the product of 7.8 MeV deuteron bombardment of molybdenum metal foil, this 4.35 days activity in Tc was identified by lifetime measurement. The normal spectrum (not shown) shows gamma lines at energies 0.14, 0.82, and 1.1 MeV. In the sum spectrum, shown in Figure 23, new lines appear at 1.65, 1.93, 2.42, and 2.69 MeV. This may be interpreted as follows. The 2.7 MeV line is the sum of 1119, 842, and 771 keV lines. The 2.42 MeV line is the sum of 806, 842, and 771 keV lines. The 1.93 MeV line is the sum of 1119, and 842, or 771 lines. And the 1.65 MeV line corresponds to the sum of any two of the 771, 806, and 842 keV lines. The 312 keV gamma is too weak to be detected. The 0.14 MeV line resulted from the decay of Tc^{99m}, the daughter product of Mo⁹⁹. Hence the 0.82 MeV line comprises also the 0.74 and 0.78 MeV gamma rays from Mo⁹⁹. Since the source was weak, it can not be definitely decided whether there are other cross-over transitions besides the 1190 keV one. The partial decay scheme confirmed by the present results are drawn in solid lines in Figure 24.

Heydenburg and Temmer found a 2 + level at 778 keV in Mo⁹⁶ by coulomb excitation. This corresponds to the first excited state in our

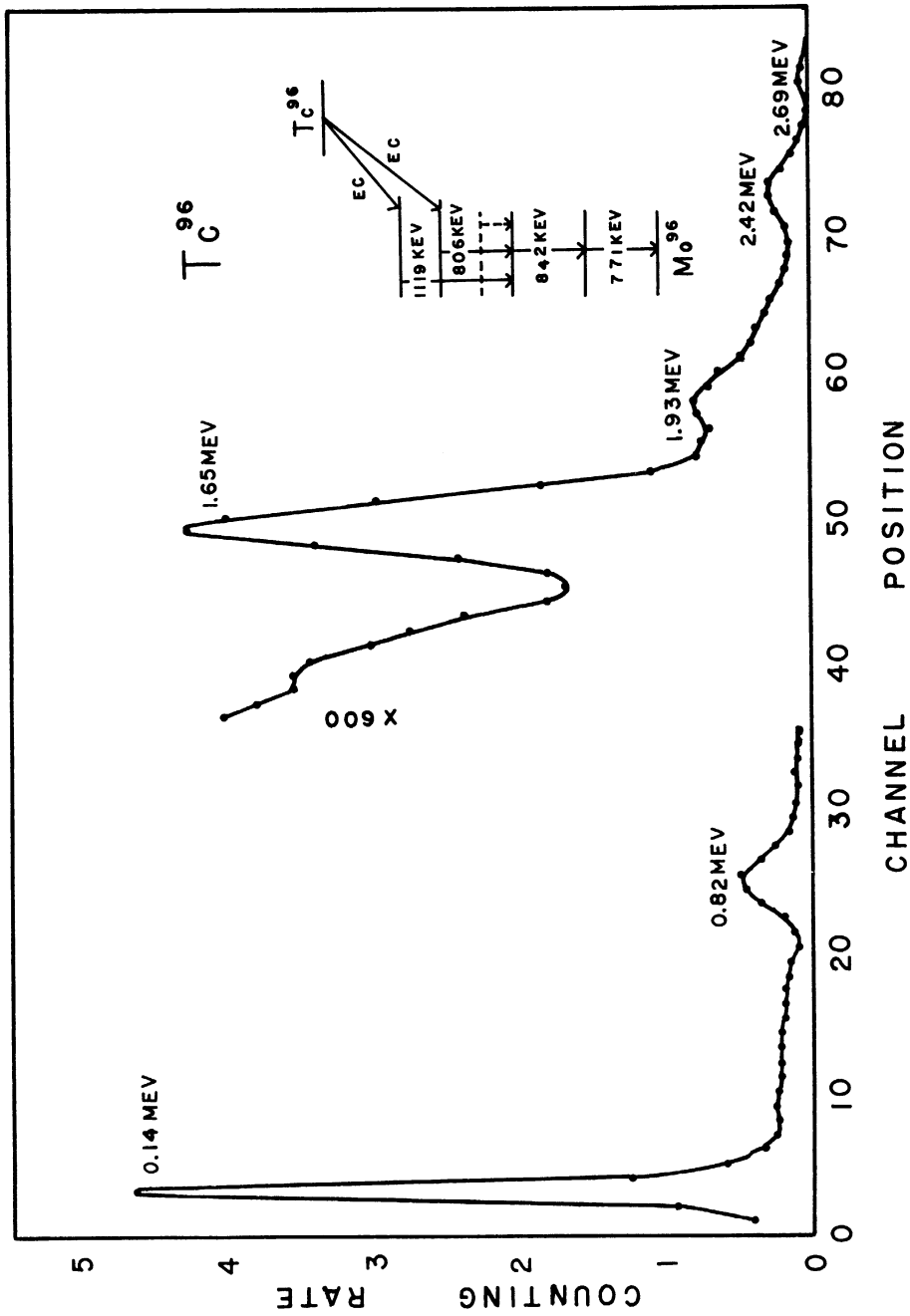


Figure 23. The Sum Gamma Spectrum of Tc^{96}

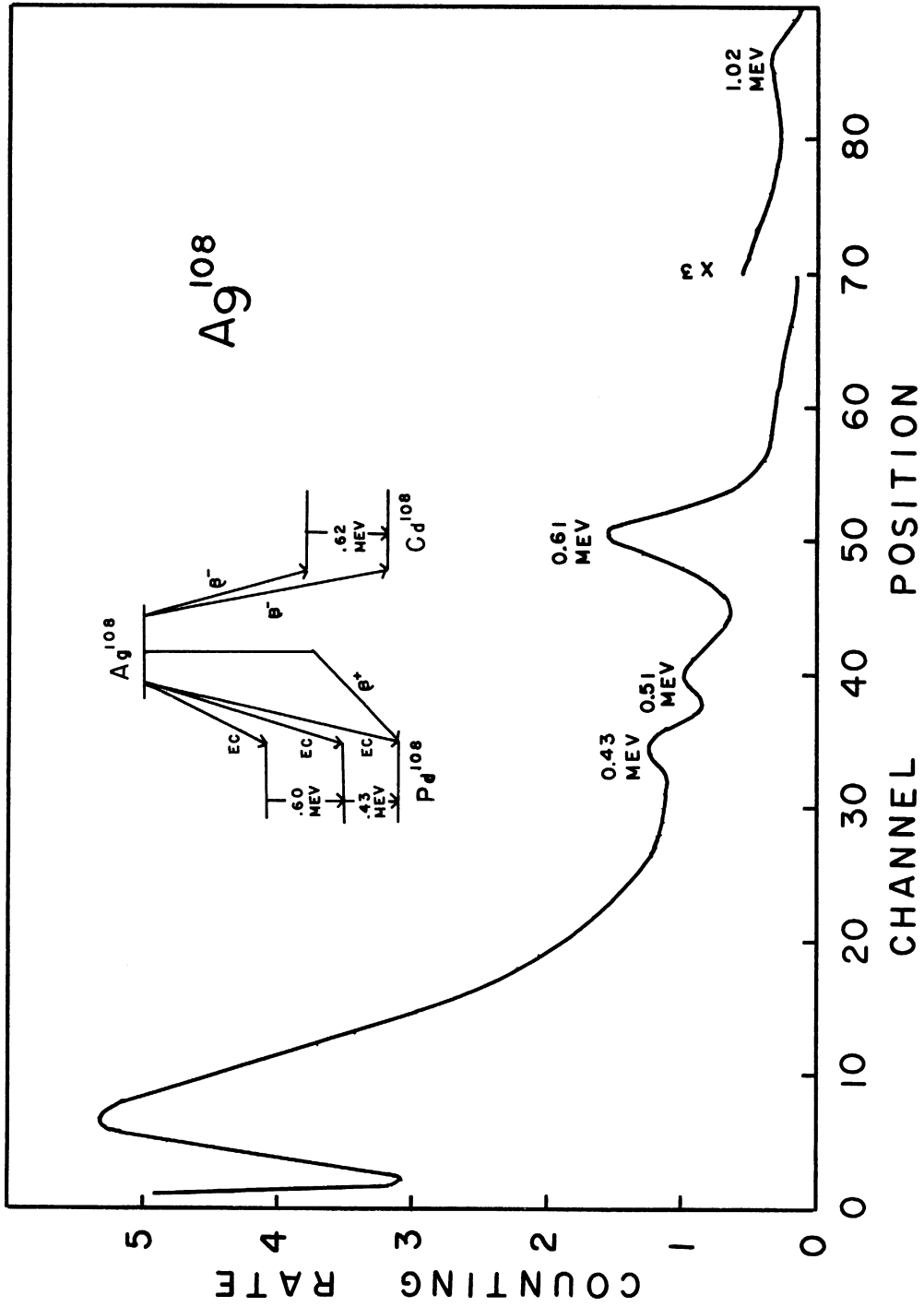


Figure 24. The Normal Gamma Spectrum of Ag^{108}

decay scheme. We may expect that the first three excited levels are vibrational in origin. A possible assignment of spins and parities is 0^+ , 2^+ , 4^+ , 6^+ , and 4^+ , assuming that no cross-over transitions proceed from the third and fourth excited levels to lower levels.

Ag¹⁰⁸ (33)

Perlman and others examined the 2.3 minutes activity in Ag with scintillators and a coincidence gray-wedge spectrometer. They found three gamma rays at energies 435, 510, and 612 kev. Coincidence measurements indicated that a 602 kev gamma ray is in coincidence with the 435 kev gamma ray. The dual nature of the decay was confirmed by x-ray-gamma-ray and beta-gamma ray coincidence measurements. We produced this activity by slow neutron irradiations of Ag₂O. The reported gamma rays were observed with the same lifetime of about 2.3 minutes. The occurrence of a new line at 1.02 mev in the sum spectrum (figure 25) leads to the conclusion that the 0.43 and 0.61 mev gamma rays are in coincidence and the 0.51 mev line corresponds to positron emission, since the relative intensities of the three lines were not appreciably affected by summing. No summing was noticed between the 0.51 mev line and other lines. So the positron emission must lead to the ground state of Pd¹⁰⁸. The broad peak at 0.12 mev is due to the beta particles emitted, as beta transitions accounts for more than 90 per cent of the decay.

The two daughter nuclei Cd¹⁰⁸ and Pd¹⁰⁸ are even-even. We expect their ground state characters to be 0^+ . Without conversion data we can not be certain about the characters of the excited levels.

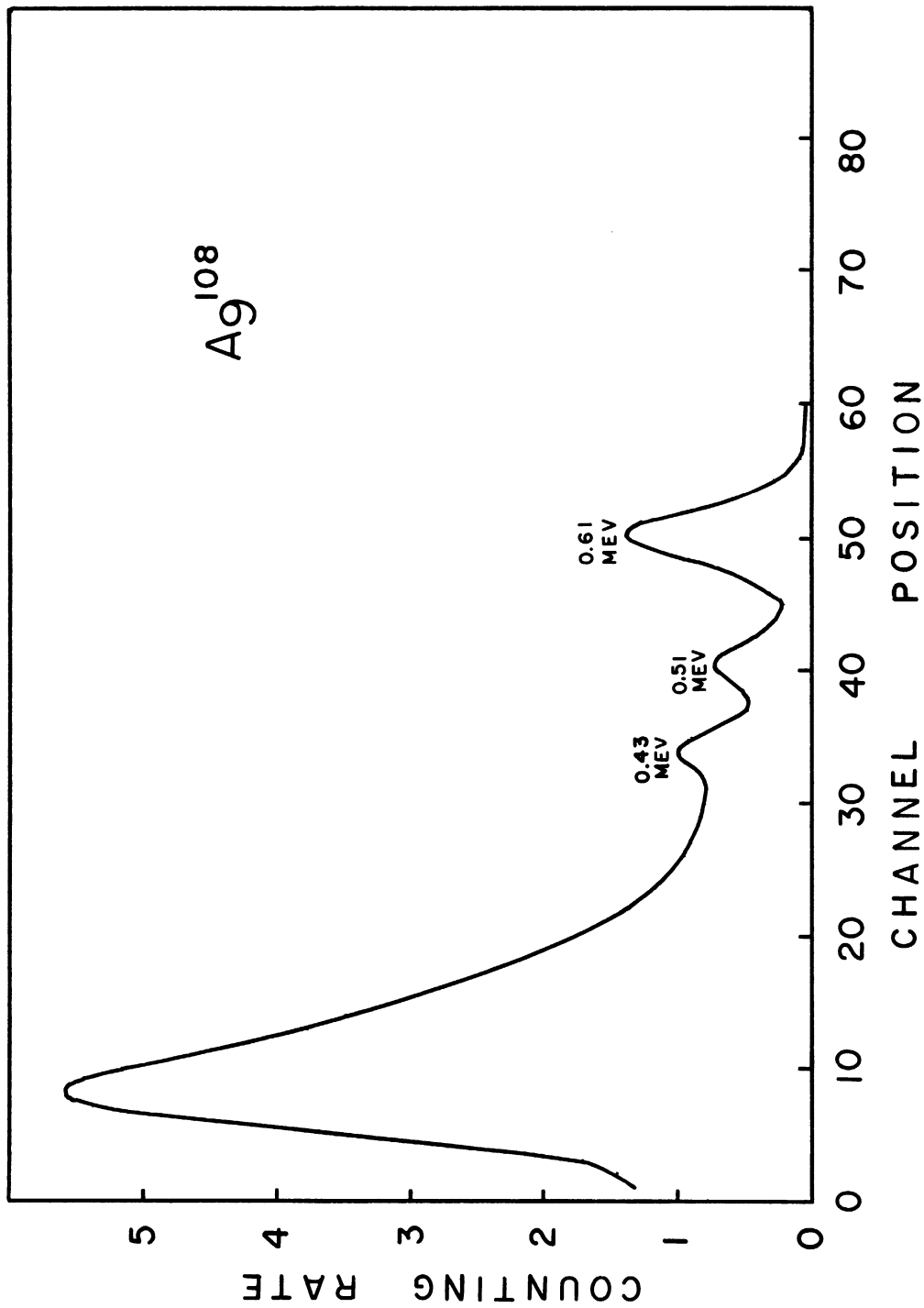


Figure 25. The Sum Gamma Spectrum of Ag¹⁰⁸

Sm¹⁵³ (18,9)

The source was supplied by Oak Ridge National Laboratory.

In a preliminary run, no prominent peaks could be seen beyond 170 kev in the sum spectrum. Efforts were made to suppress the 42 kev K x-ray arising from the conversion of the 70 kev transition. It was then found the 1/16 inch thick copper suffices to serve the purpose. Only the sum spectrum is shown (figure 26, the high energy part of the sum spectrum as insert). Since the high energy gamma rays are very weak compared to the 100 kev gamma ray, gain instability of the photomultiplier made energy calibration more difficult. Extensive runs show that sum peaks exist at 0.63 and 0.71 mev, and that the 0.175 mev peak is strengthened. In the normal spectrum five peaks are present at 0.07, 0.10, 0.175, 0.53, and 0.60 mev. Various investigators seem to agree on the existence of levels at 100 and 170 kev in Eu¹⁵³. From coincidence measurements with solid scintillators, Dubey and others deduced the existence of another level at 700 kev. They proposed a decay scheme for Sm¹⁵³, and discussed the spin and parity of each level on basis of shell model. The level scheme proposed by them is shown in Figure 26 and agrees with our results.

By means of coulomb excitations Heydenburg and Temmer found two rotational levels at 102 kev and 171 kev in Eu¹⁵³. Subsequent work on the decay of Gd¹⁵³ to Eu¹⁵³ also fails to give evidence of such excited levels. We recall that in the decay of Dy¹⁶⁵ the first rotational level at 94 kev is not reached from the upper states by gamma transitions. The explanation of this apparent disagreement may be found by actually

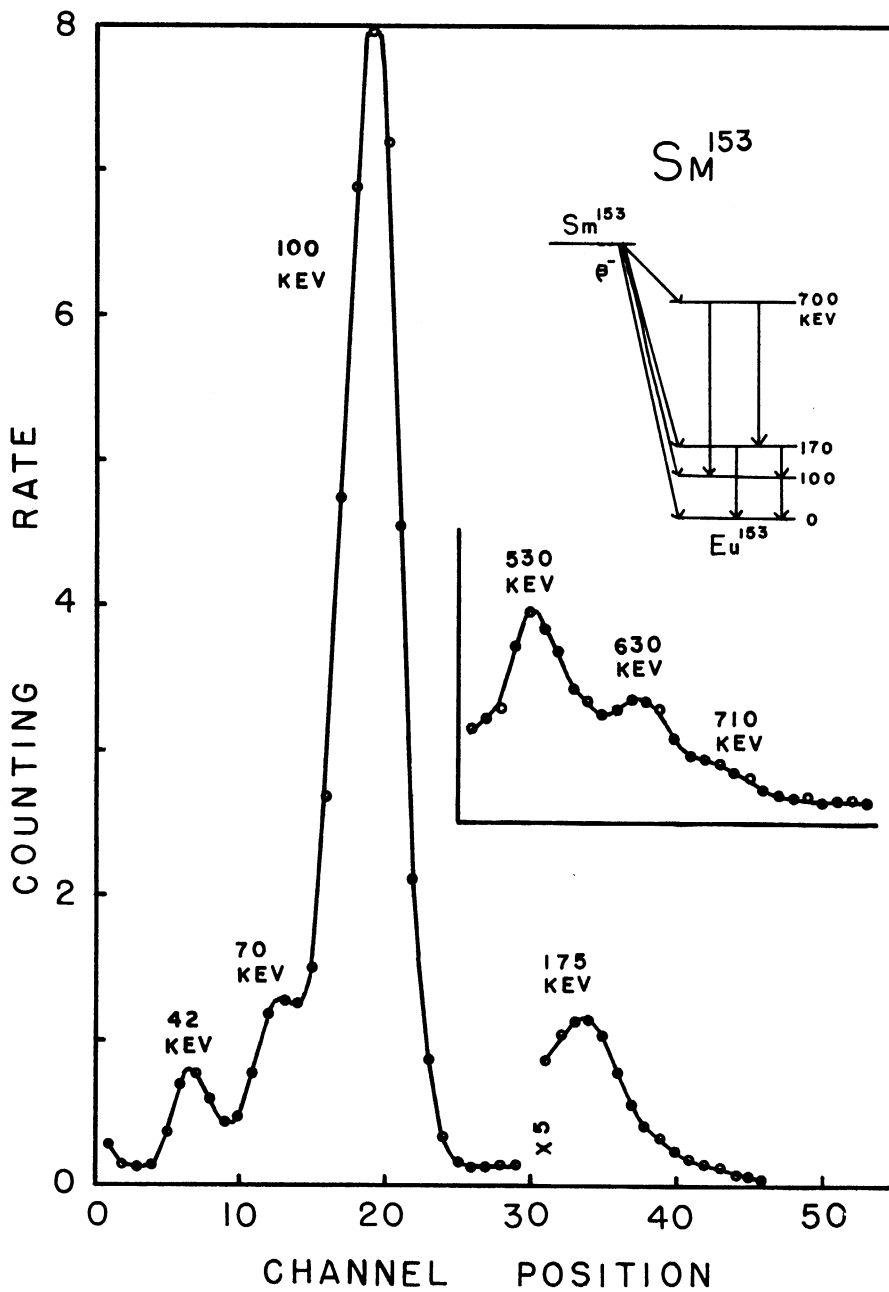


Figure 26. The Normal and Sum Gamma Spectrum of Sm^{153}

evaluating the transition probability from a level arisen from particle excitation to one arisen from collective excitation.

Conclusions

The single crystal gamma-summing method has the following advantages: (a) The energy levels of the daughter isotope are represented in the sum spectrum by sum peaks, if they do not decay directly to the ground level; if they decay both to the ground level and an excited level, the photo-peak corresponding to the ground transition will be enhanced. In any case, this method is simple in identifying the energy levels of the daughter isotope. (b) The coincidence rate is increased over that of the two-counter coincidence method, because the solid angle subtended by the counter is nearly 4π . (c) The number of electronic components is minimized and therefore, there is less chance of error. In spite of these, this method has never been widely used in nuclear spectrometry. The chief obstacle is the fact that NaI crystal is not suited for analysis of complex spectra. In the decay of heavy isotopes, a 1% energy resolution is often needed to resolve all gamma lines. (Energy resolution is defined as the ratio between the half-width of the line to its energy.) The best resolution for NaI is 6-8% for the 662 keV line of Cs^{137} . Besides, the Compton distribution obscures the low energy part of spectra. It is hopeful that a liquid scintillator can be found with all the good features of NaI crystal and yet superior as regards resolving power.

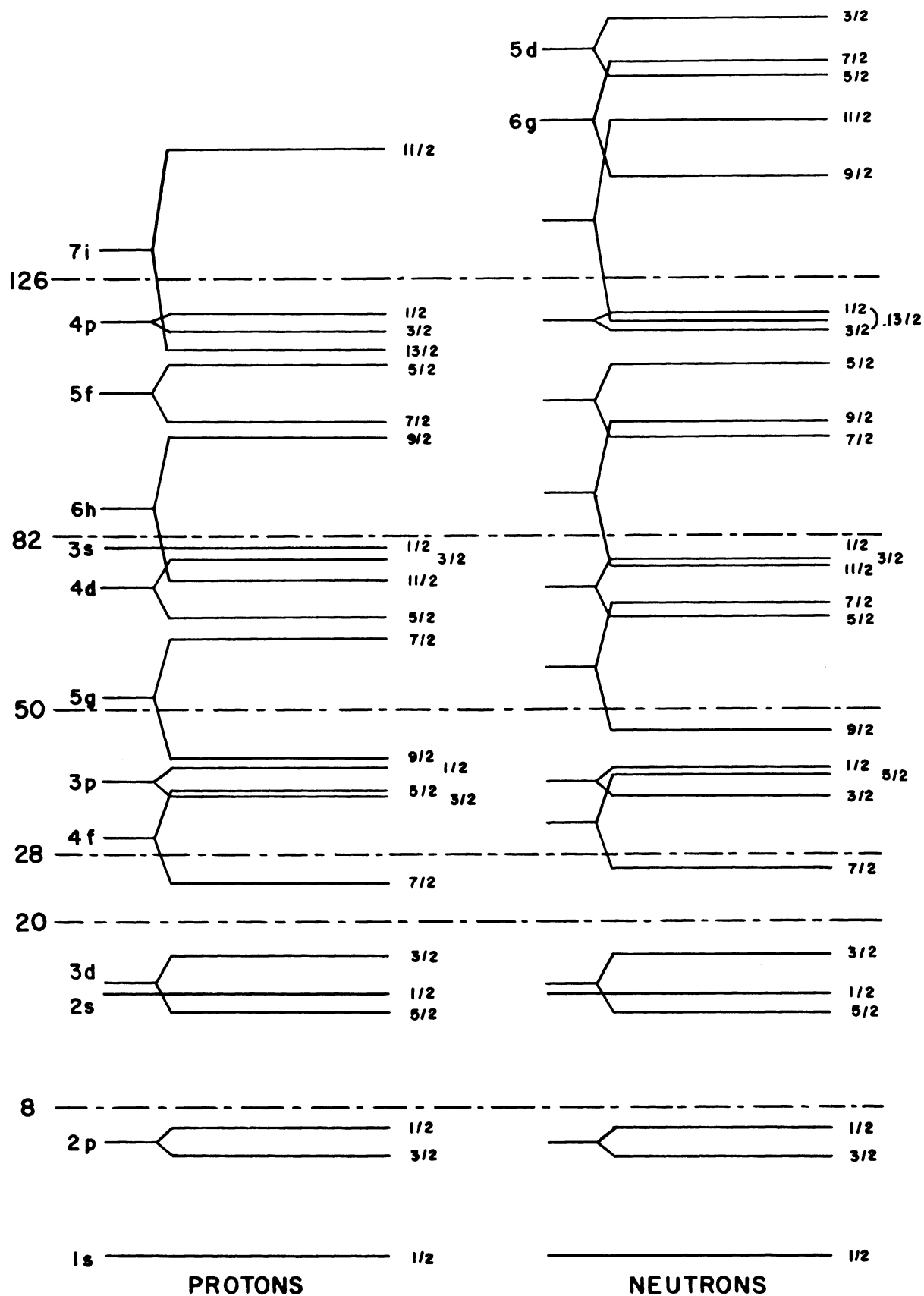


Figure 27. Single Particle Shell Scheme

BIBLIOGRAPHY

1. E. H. Bellamy and R. G. Moorhouse, Proceedings of the 1954 Glasgow Conference on Nuclear and Meson Physics, Pergamon Press, London, 195 (1955).
2. Bethe and Morrison, Elementary Nuclear Theory.
3. J. B. Birks, Scintillation Counters, McGraw-Hill (1953).
4. A. Bisi, E. Germagnoli and L. Zappa, Nuovo Cimento 10 (2), 1052 (1955).
5. Blatt and Weisskopf, Theoretical Nuclear Physics, John Wiley and Sons (1952).
6. A. Bohr and B. R. Mottelson, Dan, Mat. Fys. Medd. 27 No. 16 (1953).
7. J. M. Cork, M. K. Brice, and E. C. Schmid, Phys. Rev., 99, 703 (1955).
8. A. G. Dmitriyev, P. P. Zarubin, Izvest. Akad. Nauk. Ser. Fiz. SSSR 18, 580 (1954).
9. V. S. Dubey, C. E. Mandeville and M. A. Rothman, Phys. Rev. 103, 1430 (1956).
10. J. V. Dunworth, Rev. Sci. Instrum. 11, 167 (1940).
11. Easterday and Medicus, Phys. Rev. 89, 752 (1953).
12. Elmore and Sands, Electronics, McGraw-Hill (1949).
13. G. F. J. Garlick and G. T. Wright, Proc. Phys. Soc. B65, 415 (1952).
14. Goldhaber and Hill, Rev. Mod. Phys. 24, 179 (1952).
15. M. A. Grace, G. A. Jones and J. O. Newton, Phil. Mag. 1, 363 (1956).
16. H. E. Handler and J. R. Richardson, Phys. Rev. 102, 833 (1956).
17. W. Heitler, The Quantum Theory of Radiation, Clarendon Press (1954).
18. Heydenburg and Temmer, Phys. Rev. 104, 981 (1956).
19. W. A. Higinbotham, Rev. Sci. Instr. 22, 429 (1951).
20. J. M. Hollander, I. Perlman, G. T. Seaberg, Rev. Mod. Phys. 25, 469 (1953).

21. C. W. Johnstone, *Nucleonics* 11 36, (1953).
22. Jonker, van Overbeek and de Beurs, *Philips Research Report* 7, 81, (1952).
23. W. C. Jordan, J. M. Cork and S. B. Burson, *Phys. Rev.* 92 1218 (1953).
24. L. E. Killion, Washington University, *Dissertation Abstracts* 15, 858 (1955).
25. P. Klinkenberg, *Rev. Mod. Phys.* 24 63 (1952).
26. H. R. Lemmer, O. J. A. Segaert and M. A. Grace, *Proc. Phys. Soc.* 68A, 701 (1955).
27. D. Lu, Thesis, University of Michigan (1954).
28. Mayer and Jensen, *Elementary Theory of Nuclear Shell Structure*, John Wiley and Sons (1955).
29. H. Medicus, A. Mukerji, P. Preiswerk and G. De Saussure, *Phys. Rev.* 74, 839 (1948).
30. H. Medicus, P. Preiswerk and P. Scherrer, *Phys. Acta.* 23, 299 (1950).
31. H. Morinaga and E. Bleuler, *Phys. Rev.* 103, 1423 (1956).
32. W. Pauli, *Handbuch der Physik*, 2. Aufl., Band 24, P. 220.
33. M. L. Perlman, W. Bernstein and R. B. Schwartz, *Phys. Rev.* 92, 1236 (1953).
34. Pohm, Lewis, Talboy, and Jensen, *Phys. Rev.* 95, 1523 (1954).
35. R. F. Post, *Nucleonics* 10 No. 6, 56 (1952).
36. J. M. Reid and I. F. Wright, *Nature* 175, 298 (1955).
37. *Rev. Mod. Phys.* 29 (1957).
38. M. E. Rose, *Multiple Fields*, John Wiley and Sons (1955).
39. A. E. Ruark and F. E. Brammer, *Phys. Rev.* 52, 322 (1937).
40. G. Scharff-Goldhaber, 90, 587 (1953).
41. Scharff-Goldhaber and Weneser, *Phys. Rev.* 98, 212 (1955).

42. Siegbahn, Beta- and Gamma-ray Spectroscopy
43. P. Stahelin and P. Preiswerk, Nuovo Cimento 10 (9), 1219, (1953).
44. Temmer and Heydenburg, Phys. Rev. 104 967 (1956).
45. Wilets and Jean, Phys. Rev. 102, 788, (1956).
46. G. Wilkinson, Phys. Rev. 80 495 (1950).

UNIVERSITY OF MICHIGAN



3 9015 02829 5742